Review Article

Ismail Barbaros, Yongmin Yang*, Babak Safaei*, Zhicheng Yang, Zhaoye Qin, and Mohammed Asmael

State-of-the-art review of fabrication, application, and mechanical properties of functionally graded porous nanocomposite materials

https://doi.org/10.1515/ntrev-2022-0017
received September 26, 2021; accepted November 15, 2021

Abstract: Functionally graded porous (FGP) nanocomposites are the most promising materials among the manufacturing and materials sector due to their adjustable physical, mechanical, and operational properties for distinctive engineering applications for maximized efficiency. Therefore, investigating the underlying physical and materialistic phenomena of such materials is vital. This research was conducted to analyze the preparation, fabrication, applications, and elastic properties of functionally graded materials (FGMs). The research investigated for both porous and nonporous synthesis, preparation, and manufacturing methods for ceramics, metallic, and polymeric nanocomposites in the first section, which is followed by deep research of the development of elastic properties of the above-mentioned materials. Main nano-reinforcing agents used in FGMs to improve elastic properties were found to be graphene platelets, carbon nanotubes, and carbon nanofibers. In addition, research studied the impact of nano-reinforcing agent on the elastic properties of the FGMs. Shape, size, composition, and distribution of nano-reinforcing agents were analyzed and classified. Furthermore, the research concentrated on modeling of FGP nanocomposites. Extensive mathematical, numerical, and computational modeling were analyzed and classified for different engineering analysis types including buckling, thermal, vibrational, thermoelasticity, static, and dynamic bending. Finally, manufacturing and design methods regarding different materials were summarized. The most common results found in this study are that the addition of reinforcement units to any type of porous and nonporous nanocomposites significantly increases materialistic and material properties. To extend, compressive and tensile stresses, buckling, vibrational, elastic, acoustical, energy absorption, and stress distribution endurance are considerably enhanced when reinforcing is applied to porous and nonporous nanocomposite assemblies. Ultimately, the review concluded that the parameters such as shape, size, composition, and distribution of the reinforcing units are vital in terms of determining the final mechanical and materialistic properties of nanocomposites.

Keywords: nanocomposites, functionally graded material, porous material, synthesis, fabrication, mechanical properties

*** Corresponding author: Yongmin Yang,** College of Urban and Rural Construction, Zhongkai University of Agriculture and Engineering, Guangzhou 510225, China, e-mail: yangyongmin@zhku.edu.cn
*** Corresponding author: Babak Safaei,** Department of Mechanical Engineering, Eastern Mediterranean University, Famagusta, North Cyprus via Mersin 10, Turkey; Department of Mechanical Engineering Science, University of Johannesburg, Gauteng 2006, South Africa, e-mail: babak.safaei@emu.edu.tr
Ismail Barbaros, Mohammed Asmael: Department of Mechanical Engineering, Eastern Mediterranean University, Famagusta, North Cyprus via Mersin 10, Turkey
Zhicheng Yang: College of Urban and Rural Construction, Zhongkai University of Agriculture and Engineering, Guangzhou 510225, China
Zhaoye Qin: Department of Mechanical Engineering Science, University of Johannesburg, Gauteng 2006, South Africa; State Key Laboratory of Tribology, Department of Mechanical Engineering, Tsinghua University, Beijing, China

1 Introduction

Nowadays, the manufacturing sector is evolving rapidly, and raw material demand is proportionally increasing. To tackle this, nanocomposite material usage has started to gain a reputation in many engineering sectors [1]. Nanocomposites are noncrystalline materials that are accepted as composites, which include nanoparticles of a material of dimensions smaller than 100 nm [2]. Utilizing nanocomposites

as nanobuilding blocks establishes brand-new materials with exceptional flexibility and enhanced physical features [3]. This study deeply analyzes different porous and nonporous nanocomposites and the main reinforcing units preferred to manufacture nanocomposites. The production process of a reinforced nanocomposite consists of adding reinforcement units (mainly as a form of nanofibers or nanotubes) to any composite materials [4]. To add, since different nanocomposite types have different structures, candidate reinforcing agents are required to be selected carefully to create a valuable chemistry between nanocomposites and reinforcing units. Nanocomposites are further divided into three main groups, which are [2,5] as shown in Table 1. Furthermore, processing and manufacturing methods of porous and nonporous nanocomposites (which will be discussed later in detail) play very important role in terms of acquiring demanded mechanical properties. Even though the main manufacturing methods are generally the same for every type of porous and nonporous nanocomposites, processing and synthesis procedures vary slightly and vastly for nonporous nanocomposites and porous nanocomposites, respectively.

1.1 Recent development of elastic properties of functionally graded porous (FGP) nanocomposites

In terms of materials sector, FGP materials can be cited as a prevalent example of development in the materials industry, which are specifically engineered to get utilized in many sectors [6]. This reputation of FGP nanocomposite materials is due to their incredible high surface area to volume ratio of consolidating phase. Toward the end of twentieth century, many initial prototypes of functionally graded material (FGM) were designed as thermal insulation coatings [7]. Nowadays, FGP nanocomposite materials are obtained *via* nanoscale addition of consolidation materials, which are generally carbon nanotubes (CNTs) and graphene platelets (GPLs) into metal, ceramic, or polymer matrices [8,9]. The addition of CNTs and GPLs considerably improves energy absorption properties of thin-walled rings, arches, beams, and plates [10,11]. Additionally, such materials have become commonly selected for a wide range of engineering applications such as lightness, electrical conductivity, energy absorption, and thermal management [12]. The unique physical and materialistic properties of FGP materials come from their specifically adjusted composition or microstructure shape toward specific operations. In an engineering aspect, developing of FGPs was specifically required to reduce the stress fluctuations observed in composite materials. Moreover, FGPs exhibit decreased transverse and in-plane stresses, minimized residual stress, elevated thermal resistance, minimized thermal conductivity, and elevated fracture toughness and resistance to interlaminar stresses [13,14].

However, detailed analysis performed by Yas and Rahimi [15] on FGP nanocomposites particularly on weight fraction, scattering patterns, size and geometry of platelets, and porosity allocation and coefficient revealed that the operation performance of GPLs is highly dependent on their geometry. Free vibration, buckling, and bending analysis of FG graphene nanoplatelets (GNPs)-reinforced nanocomposite under hygro-thermo-mechanical loads were presented by Yas and Rahimi [15]. Results highlighted that the assembly gets stiffer as the weight fraction of the GNPs increases, leading to an additional increase in the natural frequency and critical buckling stress. Elevated temperature and moisture decrease the stiffness, natural frequency, and critical buckling load [16]. Safaei *et al.* [17] conducted a research to investigate the effects of CNTs and porosity properties of CNT cluster/polymer porous nanocomposite sandwich plates (PNSPs). Additionally, mechanical and thermal stresses, geometry, elastic foundation parameters, and boundary conditions impact on the loading

Table 1: Main nanocomposites' categories. Subcategories are given under each nanocomposite and represent the order of study, which is further deduced

Ceramic matrix nanocomposites (CMNCs)	Metal matrix nanocomposites (MMNCs)	Polymer matrix nanocomposites (PMNCs)
Porous CMNCs	Porous MMNCs	Porous PMNCs
Synthesis of porous CMNCs	Synthesis of porous MMNCs	Synthesis of porous PMNCs
Synthesis of CMNCs	Synthesis of MMNCs	Synthesis of PMNCs
Schematics of synthesis	Schematics of synthesis	Pros and cons of synthesis methods
Fabrication of porous and nonporous CMNCs	Fabrication of porous and nonporous MMNCs	Fabrication of porous and nonporous PMNCs
Schematics of fabrication	Schematics of fabrication	Schematics of fabrication

distributions, and the bending of PNSPs was examined. Authors highlighted that the functional grading of the core decreases deflection. Furthermore, the utilization of 5% volume fraction CNTs indicated negligible impact on the deflection of PNSPs due to the growth of CNT clusters.

1.2 Functionally graded graphene platelet-reinforced composites (FG-GPLRCs)

As previously mentioned, geometry is a vital issue in terms of free vibration and static bending performances of porous nanocomposites. Liu *et al.* [18] developed a design to investigate the weight fraction and geometry of FG-GPLRC spherical shells. Researchers created five distinctive models that have different GPL distributions, which are named as functionally ungraded, functionally grading type O (FG-O), functionally grading type X (FG-X), functionally grading type V (FG-V), and functionally grading type A (FG-A) and are displayed in Figure 1 [18].

As highlighted by the investigators, in terms of free vibration, the models FG-A (Figure 1, bottom right), FG-O (Figure 1, top right), and FG-X (Figure 1, top center), respectively, indicated an increase in the natural frequency magnitudes of torsional mode, breathing mode, and fundamental mode more efficiently. Nevertheless, in terms of static bending properties, the smallest radial displacement was observed on model FG-X (Figure 1, top center). Model FG-V (Figure 1, bottom left) possessed the lowest stress levels when different model assemblies of FG-GPLRC spheres were tested under a steady pressure acting from outside of the assembly.

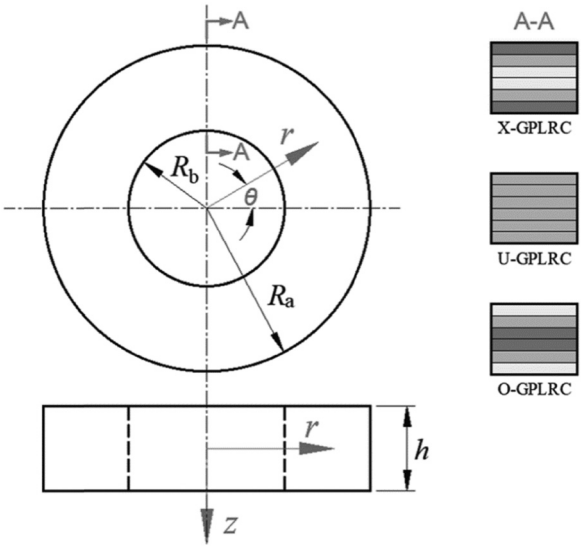

Figure 2: Geometry of FG-GPLRC multilayer annular plates [19].

As shown in Figure 2, a FG-GPLRC multilayer annular plate with an outer radius R_a, an inner radius R_b, and a thickness h is declared. The plate is reinforced of GPLs either uniformly distributed (U) or functionally graded (X and O) across the thickness. The dispersion type X with more amount of GPLs at the outer layers promotes higher linear frequency, followed by the types U and O. Contrarily, a conflicting tendency is detected for the nonlinear frequency ratio. The increase in temperature leads to an increase in nonlinear frequency ratio, however, decreased the linear frequency; those impacts were most considerable, consecutively, in type X, U, and O [19].

The impact of composition proportions on the elastic properties of functionally graded carbon nanofibers (CNFs)/

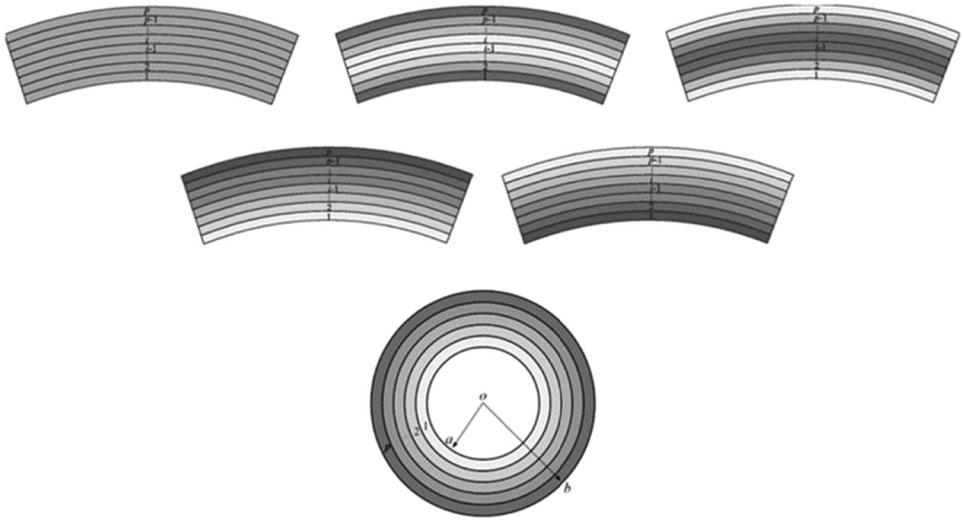

Figure 1: Geometric shell configuration [18].

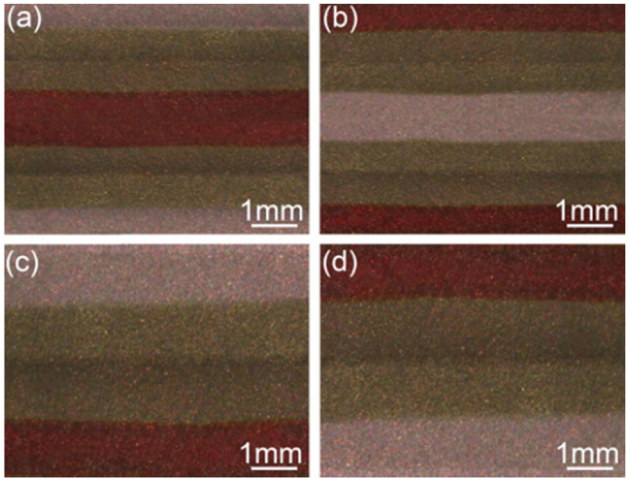

Figure 3: Optical images of the polished cross section: (a) FGN-1, (b) FGN-2, (c) FGN-3, and (d) FGN-4 [20].

phenolic nanocomposites that were manufactured *via* combination of compression molding and powder stacking was scrutinized by Bafekrpour *et al.* [20]. Functionally graded nanocomposites (FGN) were designed to have eight layers with same thickness, two layers with 0 weight fraction, wt%, CNFs; two layers with 2 wt% CNF; two layers of 4 wt% CNF; and two layers of 16 wt% CNF. Four specimens were designed, which are FGN-1, FGN-2, FGN-3, and FGN-4 (Figure 3). FGN-1 was designed to have 16 wt% CNFs at the top and bottom of the beam, and mass fraction was decreased toward the center. FGN-2, 16 wt% CNF at the center and 0 wt% CNF at the top and the bottom. FGN-3, 16 wt% CNF at the top, 0 wt% CNF at the bottom, FGN-4 was designed to have 16 wt% CNF at the bottom, and 0 wt% CNF at the top. Investigators utilized finite element as well as analytic modeling to review composition-related variances on boundary conditions, loadings, and elasticity properties of nanocomposites. The authors concluded the dependency of elastic properties of the structure on the CNFs content of the thickness of the assembly. The investigation used a high proportion of CNFs parts, which have proven to improve Young's modulus; however, the Young's modulus of the final complete nanocomposite assembly still remained low even though building parts of the assembly have high CNF content. Kumar *et al.* [21] mentioned the consolidation of the structure by using CNFs is dependent on CNFs aspect ratio, balanced dispersion, CNFs misalignment [22], end-effects, and interlaminar bonding strength. Thermal residual stresses occurred during manufacturing are reported to have an impact on the overall mechanical features of the assembly [20,23]. Bafekrpour *et al.* [20] studied the tensile stress–strain and deflection curves of distinctive functionally graded nanocomposites and nongraded nanocomposites. The results highlighted that functionally graded nanocomposite with the highest CNF content (16 wt%) showed the best flexural properties, especially, the highest stiffness, whereas the nongraded nanocomposite exhibited the highest fracture load. This was explained by the reduction of toughness when high content of CNFs was utilized. Moreover, Mishra *et al.* [24] concluded the vitality of morphology of nanoparticles on determining the elastic properties. Flexural strength and modulus are highly dependent on the direction of the exerted load. In addition to this, spherical nanoparticles offer higher flexural strength while nanorods give higher flexural modulus to the structure.

1.3 FGP graphene platelet-reinforced nanocomposites

Chen *et al.* [25] have studied especially the nonlinear vibration and postbuckling load of multilayer FG-GLPRC beams. Porosity and reinforcement distribution were kept constant in each layer while the porosity coefficient and reinforcement weight fraction were varied for every layer.

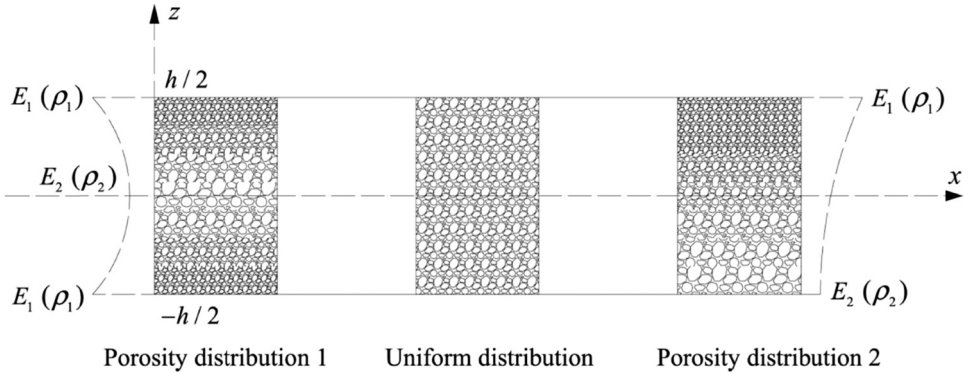

Figure 4: Three distinct porosity distributions [25].

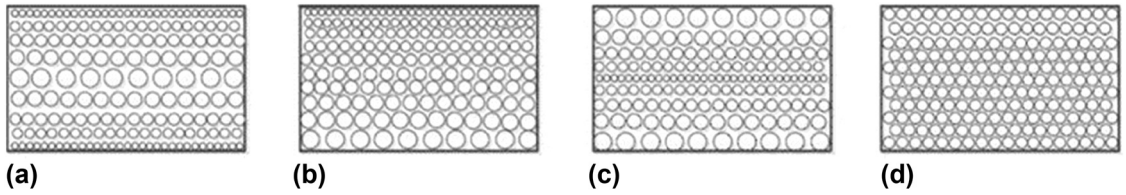

Figure 5: Distinctive porosity distributions of functionally graded porous graphene platelet reinforced nanocomposites (FGP-GLPRC) in different styles [26].

The study was carried out investigating three different porosity distributions depicted in Figure 4, which includes both uniform and nonuniform porosity distributions. E_1 and r_1 are the highest Young's modulus and mass density, respectively. E_2 and r_2 are the lowest Young's modulus and mass density of the structure, respectively. The straight lines located at the top and the bottom indicate the intersection of the E, r_1 and E_2, r_2 with the corresponding pore size distribution of both uniform and nonuniform distributions. It is vital to emphasize the highest Young's modulus and mass density values for nonuniform porosity cases (1 and 2) correspond to locations where porosity is more uniformly scattered. Additionally, for the steady porous distribution case, the middle plane was found to be the lowest magnitude of Young's modulus and mass density and also the most vulnerable to stresses.

Another study carried out by Xu *et al.* [26] investigated the acoustical characteristics of the FGP graphene-reinforced nanocomposite plates. Different porosity and graphene distributions were used. Figures 5 and 6 have been added to illustrate both porosity and GPL distribution inside the nanocomposite assembly.

Investigation concluded the dependency of the acoustic properties on both porosity and reinforcement distribution such that the porosity considerably impacts stiffness, which has a direct influence on sound transmission loss values. Additionally, the impact of separation of reinforcement units (GPL) within the nanocomposite structure has been found to be controlling parameter in terms of acoustical features [26]. Moreover, different porous structures of cylindrical shells to find critical buckling values have been studied. Results concluded that the symmetrical distribution of the pores and GPLs through the thickness of the cylindrical shell proposes the optimal buckling values, whereas the physical size of the pores is inversely proportional with the buckling features of the structure [27].

Figure 7 obtained from an earlier study [28] illustrates the effect of distinctive porosity distributions (*i.e.*, even and uneven) on deflection abilities of a square plate. Where w_{adim} being the centralized deflection, which is the ratio of the central transversal displacement w, to the plate thickness h, ($w_{\text{adim}} = w/h$). Moreover, load parameter, donated by P is defined by the formula $q_0 a^4/E \times h^4$, where q is generalized nodal displacements vector, a is the square length, E is the Young's modulus, and a is the porosity volume fraction where $0 < a < 1$. The research concludes higher displacement values for porous structures compared to nonporous structures. Additionally, even porosity distribution with higher a value led to the greatest displacement [28].

1.4 Effects on the reinforcement of particle stiffness, geometry, and size

The main materials used in the reinforcement of nanocomposites are GPLs and CNTs. Even if both materials offer decent levels of reinforcement in terms of mechanically, elastically, and operational life, distinctions are present between the two reinforcement types. CNTs are proven to be more efficient than GPLs in terms of mechanical reinforcement in the case of symmetrical distribution, whereas GPLs propose more efficient reinforcement when random

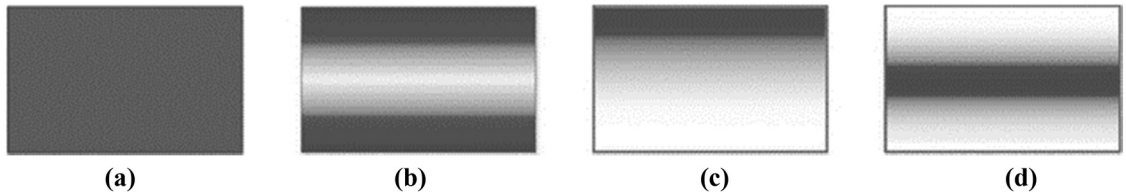

Figure 6: Distinctive GPL distribution of FGP-GLPRC in different styles [26].

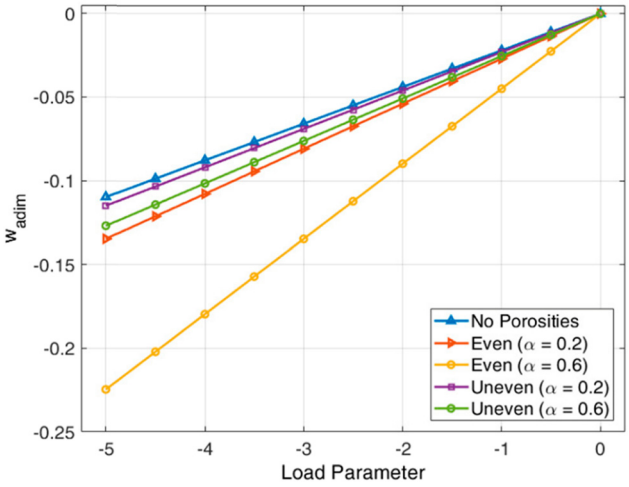

Figure 7: Effect of different porosity distributions and volume fractions on the centralized deflection [28].

distribution of reinforcement is the case. Furthermore, when the same physical magnitude and identical separation is utilized, CNTs offer considerably higher reinforcement than that of GPLs. This will cause a difference in bulk properties between CNT-reinforced and GPL-reinforced nanocomposites [29].

However, increasing the composition of soft/elastic micron/nanofillers enhances the impact toughness, however, decreases the Young's modulus. Contrarily, increasing the composition micron/nano hard/rigid filler enhances impact toughness as well as Young's modulus of polymer-based assemblies [30,31]. Additionally, the toughness and stiffness of the nanotube-reinforced polymer nanocomposites were obtained to be the functions of the elastic modulus of the nanotubes [32]. However, elastic modulus has been found to be increased slightly when the size of nanofillers utilized in the structure was decreased. Inversely, when the size of nanoparticles used in the structure decreased, the tensile strength of the structure has been found to be decreased [33]. Xu and Hoa [33] noted that the interfacial fracture toughness of carbon-fiber-reinforced epoxy/nanoclay nanocomposites was nearly doubled (85%) when four pieces of nanoclay were added to hundreds of epoxy by mass. Polit *et al.* [34] stated the impact of the weight dispersion pattern of GPLs on the stiffness, which was related to the porosity dispersion in metal foams. The places of the maximum shear stress and zero normal stress among the thickness are again related with porosity and GPLs load dispersion forms. Noteworthy variation in the buckling and fundamental frequency values was recorded when the amount of GPLs increased [35–37]. The characteristic and thickness proportion of GPLs significantly affect the operation performance of the beam. Feng *et al.* [38] studied the nonlinear static bending of multilayer functionally graded nanocomposite beams consolidated with GPLs. The study also discussed both the random and uniform distribution of GPLs. This research observed even a minor amount of GPL addition to the structure considerably decreases the static bending deflection of the beam further, this consolidation increases as the weight proportion of GPLs increases. As previously mentioned, this study also highlighted the importance of the GPL distribution pattern in terms of enhancing the bending properties of the beam. Utilizing square GPLs with less single graphene layers and distributing more GPLs close to the top and the bottom surfaces of the beam instead of uniformly over the beam thickness is the most efficient method to effectively consolidate the stiffness and to decrease the deflection of the beam [39]. The normal stress break or disparity over the thickness direction of the beam drastically enhanced by increasing the overall number of layers. Utilization of ten layers can afford a decent approximation to the chosen GPLs dispersion, significantly decreased mismatch and comparatively less manufacturing cost. Arefi *et al.* [40] mentioned the nondimensional deflection of microplate is increased when the height-over-length ratio of the GPL is increased. Similarly, increasing the thickness-over-length ratio of GPLs when the volume of the graphene content kept constant, the stiffness of the plate decreases, which causes an increase in deflection. The increase in the GPL content increased the stiffness of the plate and decreased the interfacial strains. Increased porosity coefficients increased the axial stress. Additionally, increased porosity coefficients caused the increase in deflection, stress, and strains. Table 2 summarizes the effect of different parameters such as filler composition, filler size, filler weight distribution, and filler size on the operation performance of the final product in terms of impact toughness, buckling values, vibrational characteristics, elastic modulus, tensile strength, stiffness, and various stress properties [41].

2 Processing, fabrication, and applications of different porous nanocomposites

2.1 CMNCs

CMNCs are the mixing of one or several different ceramic phases to increase the wear resistance and thermal stability. Ceramics alone suffer from low toughness that results

Table 2: Classification of different parameter impacts on the operation performance

Parameter	Impact
Increasing the composition of nano/microfillers (soft/elastic materials)	Increase in impact toughness Decrease in elastic modulus
Increasing the composition of nano/microfillers (hard/rigid materials)	Increase in impact toughness Increase in elastic modulus
Increasing the size of nanofillers	Improvement in elastic modulus
Decreasing the size of nanofillers	Decrease in tensile strength
Addition of nanoclays to carbon fiber-reinforced epoxy nanocomposites	Significant increase in fracture toughness
Weight distribution of nanofillers	Increase in stiffness
Weight fraction of nanofillers (GPLs)	Increase in stiffness Increase in critical buckling stress Increase in natural frequency
Increasing the composition of nanofiller (GPLs)	Increase in buckling values Decrease in static bending deflection (further improvement achievable *via* increasing the weight proportion of GPLs) Increase in stiffness Decrease in interfacial stresses
Increasing the amount of reinforcement (for GPL in fiber-reinforced assemblies)	Decrease in buckling load
Increasing the amount of reinforcement (for GPL in arches)	Increase in dynamic buckling load
Distribution of reinforcing particles close to the surface (GPLs)	Larger critical buckling load and postbuckling load-carrying ability
Increasing the amount of reinforcement (CNT)	Reduce in vibrational characteristics
Distribution type of nanofillers	Uniform distribution of nanofillers leads to an increase in the bending properties (including CNTs and GPLs) Uniform distribution of porosity and GPLs supports antibuckling properties
Shape of nanofillers	Using square nanofillers close to top and bottom of beam structures leads to an increase in stiffness and improves resistance to deflection
Increasing the number of layers in the laminated structures	Improvement in the stress distribution
Increasing the height-over-length ratio of rectangular nanofiller	Increase in nondimensional deflection
Increasing the thickness-over-length ratio of rectangular nanofiller	Decrease in stiffness and corresponding decrease in deflection resistance
Increasing porosity coefficients	Increase in axial stress Increase in deflection, stress, and strains
Increasing the temperature	More observable decrease in natural frequencies of functionally graded beams

in brittleness, which avoids the utilization of ceramics in many industrial applications. However, low toughness and brittleness problems are tackled when CMNCs used to offer more efficient and longer operation time at the area of utilization [2]. The reason why CMNCs are much stronger than ceramics alone lies at their structure where energy-absorbing materials such as fibers or particles are included in the ceramic matrix to decrease the brittleness and improve the durability against fracture [42]. Aluminium oxide (Al_2O_3) and silicon carbide (SiC) are the most common materials used in CMNCs. Examples of CMNCs can be given as Al_2O_3/SiO_2 and SiO_2/Ni [5,43].

2.1.1 Porous CMNCs

Porous ceramic (nano)composites offer many benefits such as minor electrical and thermal conductivity, light-weight, low heat-to-mass ratio, increased specific surface area, reasonable hardness, resistance to wear, corrosion, and high temperature applications. The mentioned improved mechanical and material properties made porous ceramics significantly common in various engineering applications [44–46]. Processing of pores, fabrication of the porous matrix, and the physical dimensions of the pores have a great impact on the mechanical and material properties of the

manufactured ceramic composites. Recent progress on the development of the pore control of the ceramics has developed a category in terms of separation of the pores with regards to their physical dimensions. International Union of Pure and Applied Chemistry (IUPAC) divided porous materials into three parts, which are represented in the descending order as macroporous (diameter, "$Ø_{macroporous}$" > 50 nm), mesoporous (50 > $Ø_{mesoporous}$ > 2 nm), and microporous ($Ø_{microporous}$ < 2 nm). Figures 8–10 illustrated the categorization together with the main applications and manufacturing techniques with respect to definite pore diameters as well as nanoscale porous structure images of open-cell and closed-cell ceramics [47–49].

Although there are many recent processing techniques of porous ceramics under development, the most obvious processing methods can be stated as partial or full sintering, replicas, sacrificial templates (fugitives), and direct foaming [47,50,51]. Although the processing techniques of the porous ceramics is slightly different from nonporous ceramics, manufacturing techniques are still the same. Especially, additive manufacturing (AM) techniques, that is, chemical vapor deposition (CVD) is the most common technique in terms of producing porous ceramic structures, which are given in Table 3.

2.1.2 Processing and synthesis of ceramic matrix nanocomposites (PCMNCs)

The most popular techniques utilized for PCMNCs and porous ceramics are powder, polymer precursor, spray pyrolysis, and chemical and physical vapor depositions. Tables 4 and 5 include visualization of some common strategies of manufacturing CMNCs. Additionally, Table 5 includes accessible schematics with labels of CMNC synthesis.

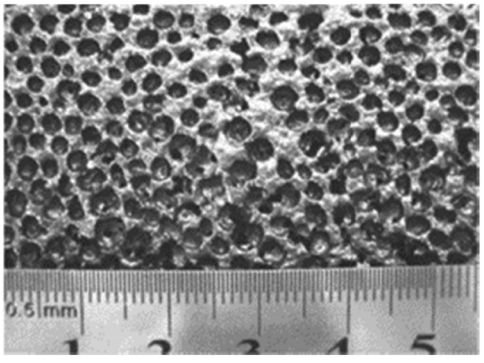

Figure 8: Porous structure of a closed-cell ceramic foam [47].

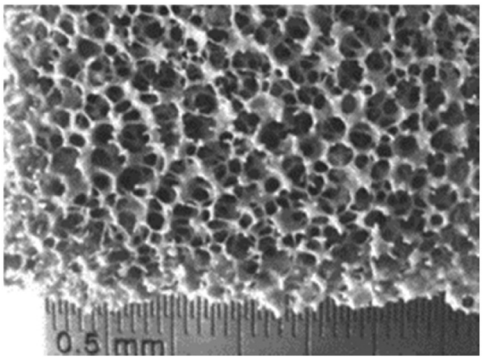

Figure 9: Porous structure of an open-cell ceramic bubble-foam [47,48].

Some main synthesis methods, such as powder, sol–gel, precursoring, and pyrolysis techniques, have their unique way of processing methods. Table 6 has been included to emphasize the order of process as well as various stages of the relative operation.

Every engineering manufacturing technique has its own advantages and disadvantages. Table 7 has been included to state and explain the relative advantages and disadvantages of the synthesizing as well as processing systems of the CMNCs mentioned above in this article.

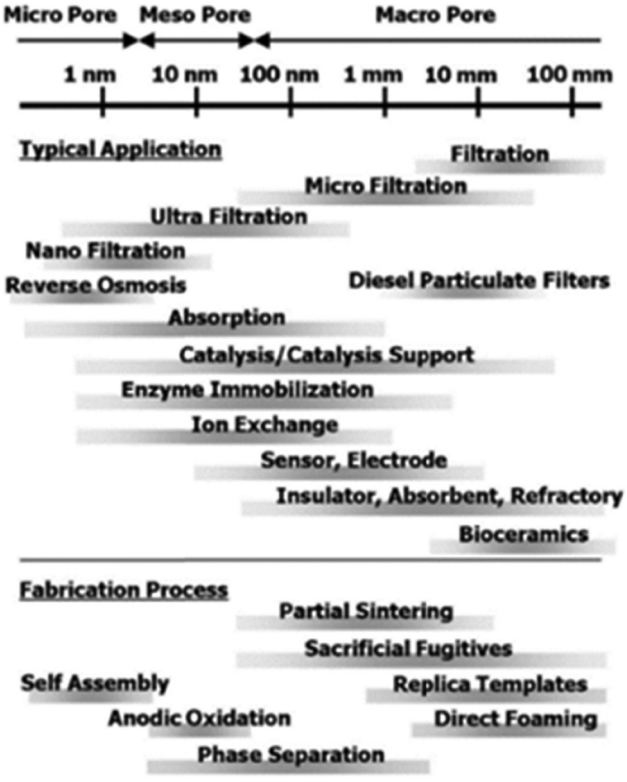

Figure 10: Categorization of different pores with relative manufacturing techniques [46].

Table 3: Processing techniques of porous ceramics

Synthesis method	Description	Ref.
Sintering	Synthesis process includes the reaction of relevant reactants with suitable precursors to obtain vapor phase nanoceramics	[47,50,51]
Replica templates	– Utilizes either synthetic or natural template, which is infiltrated through a ceramic suspension – Later, when the mix is dried off completely, the template is detached leaving a replica of the initial template morphology	[47,50,51]
Sacrificial templates, that is, *freeze casting*	– This method includes the so-called "pore former" or sacrificial to perform as a place keeper in the ceramic matrix – Once the ceramic matrix consolidates, sacrificial is detached leaving empty pores behind – To cite an example to this specific process, freeze casting uses ice crystals in ceramic matrix to form pores	[47,50–52]
Direct foaming	Utilizes gas bubbles that are intentionally trapped in the ceramic matrix during the slurry phase. When the ceramic slurry is dried off, the places occupied by gas bubbles take spherical pore shapes	[47,48,50,51]

2.1.3 Fabrication of ceramic matrix nanocomposites (FCMNCs)

Fabrication of composites, nanocomposites, and porous and nonporous ceramic matrices are the same. The different ceramic materials are obtained at the synthesizing stage with different procedures (Tables 2 and 3). However, the final fabrication method, which can be implemented to mass production is the same for every ceramic composite branches. The most common fabrication techniques for CMNCs have been determined along with every process's individual reactant arrangement and technique specification, which are presented in Table 8.

Table 8 mentions the main methods for fabrication of CMNCs. Additionally, Table 9 visualizes the above-mentioned fabricating strategies of manufacturing CMNCs. Accessible schematics with labels (if present for that process) of CMNC fabrication are presented below.

2.2 MMNCs

MMNCs are the mixing of ductile metal or alloy matrix and nanosized reinforcement materials. The cooperation between ductile metals and nanoparticles causes MMNCs to have an elevated ductility, toughness, strength, and modulus. Due to their superior materialistic and mechanical properties, MMNCs are widely utilized in automotive and aerospace industries [2]. Examples of MMNCs can be stated as iron–chromium (Fe–Cr)/Al_2O_3, nickel aluminium oxide (Ni/Al_2O_3), and Co/Cr (cobalt chromium) [5].

2.2.1 Porous MMNCs

Highly porous metals are attractive due to the high flow stress and toughness, solid mechanical formability, resistance to thermal degradation, and significant electrical and thermal conductivity features [108]. Porous structured metals are classified as lightweight, improved mechanical and material properties, with an additional energy absorption feature [109]. To be able to produce porous metals effectively and useful for specific engineering applications, various processing techniques has been recently used in the sector. Powder metallurgy, melt foaming, metallic fiber sintering, gas injection to metallic sheets, infiltration, metal deposition, and hollow sphere sintering are the main methods used for processing of porous structured metals [110]. Furthermore, lately innovated techniques to process and produce porous metallic structures are casting foaming (Aluminium foam) processes, precursor foaming, LOTUS-type foaming, and space holding processes. The most commonly utilized technique among these processes is the space holding process due to its ability in terms of allowing the regulation of the pore morphology of the porous metals [108–119]. Figure 11 shows the structure of porous aluminium (metal foam) obtained *via* space holder method. Additionally, this particular type of porosity is called a closed-cell structure, which can also be identified as metal foam. To extend, the closed-cell configuration in metals is more advantageous for many applications as it can endure under high pressure. Additionally, the closed-cell porous structures are nearly four times denser than the open-cell porous structures, which makes them more suitable for

Table 4: Indicating processing stages and synthesis methods for CMNCs

Synthesis process	Arrangement	Process	Ref.
Sol–gel	Silica oxide/nitrite (SiO_2/Ni), zinc oxide/cobalt (ZnO/Co), titanium oxide/iron(III) oxide (TiO_2/Fe_2O_3), lanthanum oxide(La_2O_3)/TiO_2, Al_2O_3/SiC, TiO_2/Al_2O_3, Al_2O_3/SiO_2, Al_2O_3/SiO_2/zirconium oxide (ZrO_2), TiO_2/iron(III) titanium oxide (Fe_2TiO_5), neodymium aluminium oxide ($NdAlO_3$)/Al_2O_3	– Addition of water and condensation reactions of an organic/inorganic molecular precursor dissolved inorganic solutions – Three-dimensional (3D) polymers that contains metal-oxygen bonds are obtained at the end of mentioned reactions – The process is followed by ventilation operation to remove excess liquids and to obtain a solid material, which is then subjected to thermal operations for strengthening	[53–57]
Powder	Al_2O_3/SiC	– Choice of materials that will be used in the process (mainly selected as powders mainly small dimensions, uniform, and purified) – Mixing of the solution in organic or aqueous solutions by using a technique called wet ball milling or a attrition and milling – Drying by utilizing lamps and special ovens or by freeze drying – Heat-treatment processes are applied to strengthen the obtained solid material. Such processes are generally hot pressing, gas pressure sintering, slip casting or injection molding, and pressure filtration	[55,56]
Polymer precursor	Al_2O_3/SiC, silica nitride/SiC	– Addition of silicon polymeric precursor to the matrix material. Pyrolysis of the solution with the help of microwaves, leading to the consolidation particles	[55,56,58]
Mechanochemical	*For oxide–oxide composites* Acid base/magnesium TiO_2, beta phase CP/magnesium TiO_2/magnesium oxide *For nonoxide–oxide composites* Al_2O_3/zirconium diboride/ZrO_2. Al_2O_3/titanium diboride *For nonoxide–nonoxide composites* Boron carbide/SiC, niobium carbide/niobium diboride	– This specific type of solid-synthesis technique includes mixing of mechanical and chemical facts at a macroscopic scale. It is feasible *via* this method to obtain a required product utilizing solely mechanical action such as the application of elevated pressure to the reactants at an ideal temperature	[59–65]
Vapor phase	*For oxide–oxide composites* ZrO_2/SiO_2, TiO_2/vanadium pentoxide *For nonoxide–nonoxide composites* Silicon nitride/SiC	– Vapor phase synthesis process includes the reaction of relevant reactants with suitable precursors to obtain vapor phase nanoceramics, which then can be deposited on the required surface easily *via* various methods such as CVD – Gas phase condensation method is also a common way of vapor phase processing	[65–68]
Self-propagating high temperature synthesis (SHS)	*For nonoxide–nonoxide composites* Silicon nitride/titanium nitride, silicon nitride/molybdenum silicide, silicon nitride/SiC, titanium nitride–silicon nitride–silicon nitride,	– Synthesis of required material is accomplished by using heat obtained from the chemical reaction of the material during processing	[65,69–73]

(*Continued*)

Table 4: *Continued*

Synthesis process	Arrangement	Process	Ref.
	zirconium diboride–SiC–zirconium carbide–zirconium silicide *For nonoxide–oxide composites;* Al_2O_3/SiC, mullite/titanium diboride	– The reacting substances will alter to resultants throughout the combustion reaction, which will be observed straight after the reaction initiates	
Spray decomposition/ (combustion)	*For oxide–oxide composites* Al_2O_3/zirconium dioxide; cerium(IV) oxide–metal$_x$oxide$_y$; and metal oxide$_x$–zinc dioxide; Gamma–iron(III) oxide–TiO_2/ZrO_2/ magnesium aluminate	– Another name of the process is solution combustion – The process includes initiation and developing of automaintained heating reactions at an either aqueous or sol–gel atmospheres – Distinctive nanomaterials can be synthesized *via* this method – Control of reaction conditions greatly affects the yield	[65,74–77]
Coprecipitation synthesis	*For oxide–oxide composites* Aluminium oxide/zirconium dioxide; aluminium oxide/yttrium aluminate; zirconium dioxide/ gadolinium oxide; lanthanum aluminium (11) oxide (18); and calcium hydroxyapatite/iron(III) oxide/mullite/aluminium oxide	– The process is considered to be an alternative to similar sol–gel processing as it is also utilized chemical ways to mix oxides together – The reaction includes dissolution of reactants in a traditional solvent and a following addition of precipitating agent to obtain a homogeneous solid material – The precipitation solution is further decomposed at elevated temperatures to obtain aimed oxide	[65,78–81]
Surface modification	*For oxide–oxide composites* Al_2O_3/ZrO_2; Al_2O_3/yttrium aluminate; Al_2O_3/ mullite; Al_2O_3/silicon dioxide; and zirconium dioxide/magnesium aluminate Al_2O_3/zirconium dioxide/yttrium aluminate Zirconium dioxide/Al_2O_3/strontium aluminium (12) oxide (19) *For oxide – non–oxide composites* SiC/Al_2O_3 SiC/yttrium oxide	– Surface-modification processes act as a bridge between powder mixing and chemical methods – The aim of the surface modification is to enhance the properties of the powders which will be used in the mixing process – This process not only increases the efficiency of the overall synthesis but offering an enhancement in terms of control of the ultimate physical and morphological condition of the obtained microstructure	[65,82–87]

harsher operations. However, comparatively high density of closed-cell structures makes them infamous for light-weight engineering applications [120,121]. Nevertheless, the processing method utilized to attain porous structure on the metallic materials decides the nature of the porous matrix. Moreover, porous structure within any metallic materials plays an important role in deciding the ultimate physical and mechanical properties. Hence, categorization of porous metals leads to a separation of the above-mentioned processing techniques into following sets [108]:

- Isolated porosity
  - Pores are isolated within the metal structure. Sometimes referred as "dilute porosity."
- True metal foam
  - A gas phase generates a group of physically in contact bubbles divided by thin metal membranes. Hence, the natural structure of the specific porous system tends to be closely celled.
- Foam precursor
  - An already located polymer foam (*i.e.*, polyurethane) is utilized to produce the structure of the metal.

Table 5: The schematic of the synthesis methods for CMNCs. The processes, which schematics are not included, are either chemical reactions or do not have any processing unit

Schematic of sol–gel processing	[88]

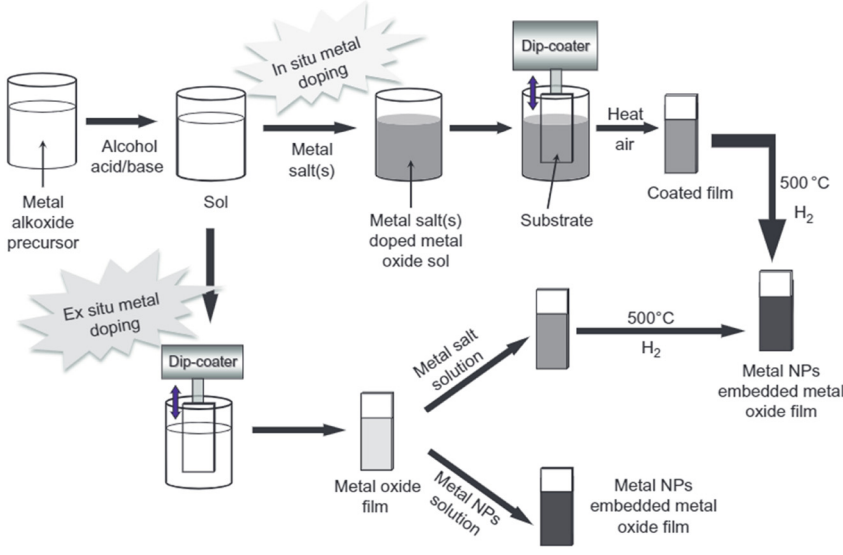

Schematics of powder processing for various materials	[89]

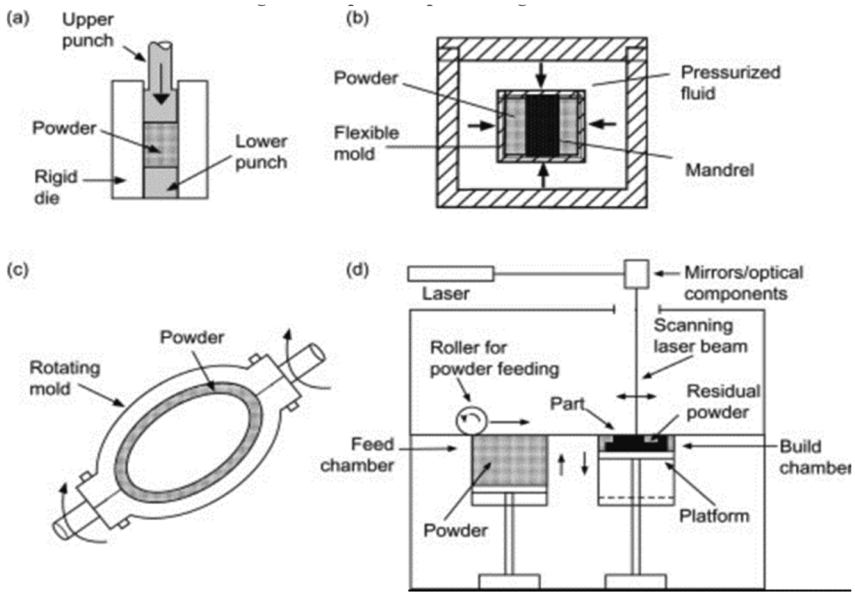

(*Continued*)

Table 5: *Continued*

Schematic of SHS unit	[90]
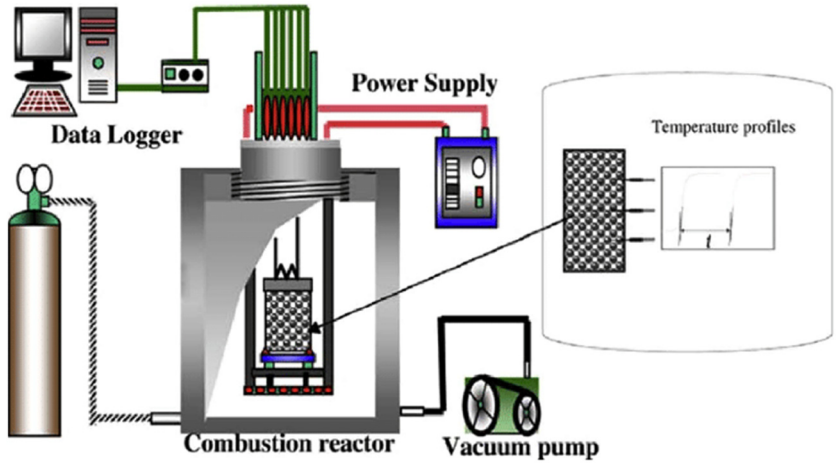	
Schematic of the spray decomposition	[91]
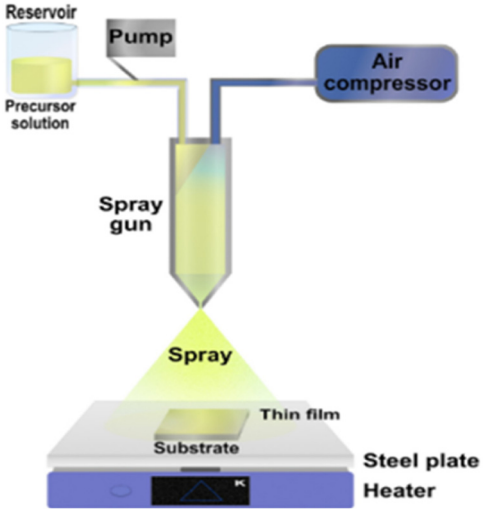	
Schematic of the coprecipitation synthesis	[92]
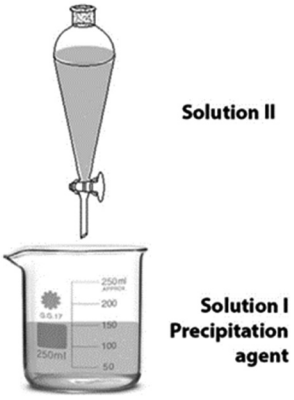	

Table 6: The processing stages for (1) powder, (2) sol–gel, (3) polymer precursor, and (4) gas phase pyrolysis obtained from an earlier study [56]

Powder (1)	Sol–gel (2)	Polymer precursor (3)	Pyrolysis (4)
Ceramic powder + nanoparticles	Ceramic precursor sol + nanoparticles	Ceramic powder + polymer	$[Si(CH_3)_3]_2NH$ + NH_3 (in air)
Ball milling (solvent)	Mixing	Coating/drying	Reaction chamber (1,000°C/N_2)
Drying	Hydrothermal processing	Coated ceramic powder	Amorphous (Si_2N_4)
Hot pressing	Sol	Cross linking	Furnace (1,500°C/6 h/argon)
	Drying	Pyrolysis	Heat treatment (1,350°C/4 h/argon)
	Hot pressing	Hot pressing	Mixing with sintering aids Hot pressing

- Porosity created by packing
  - Individual porous elements are attached together to form an assembly, which has high pore content.
- Porosity created by phase change
  - Phase changes of a single distinct phase to many phases, mainly gas, leads to the creation of a porous structure.
- Regular lattices
  - A steadily porous structure, generally created by uniform beam elements, is recurred a lot of times to generate a material.

Additionally, processing and preparation of porous metal (nano)composites is achieved *via* combined processing or reprocessing of techniques mentioned above. To cite an example, redepositing or filling of porous metals with additional porous metals or porous alloys. Either welding and bonding operations are carried out to attach porous components together or porous assemblies are created *via* addition of distinctive metal powders, fibers, and other materials, which are then transferred to the processing unit for further reprocessing with the help of techniques stated above [108–110].

2.2.2 Processing and synthesis of metal matrix nanocomposites (PMMNCs)

The most popular techniques utilized for PMMNCs and porous metals are precursoring, pyrolysis, CVD/physical vapor deposition (PVD), infiltration and solidification, and sol–gel processes. Table 10 summarizes the procedure, arrangements, and operations of every process.

Table 10 presents the main techniques during the synthesis of MMNCs. Additionally, Table 11 includes visualization of the most popular processing methods of MMNCs. Accessible schematics with labels of MMNC synthesis are also included in the table.

The following table summarizes the advantages and disadvantages of the above-mentioned processes, which are utilized for the synthesis of MMNCs. Both major and minor advantages and disadvantages are given and explained in Table 12.

2.2.3 Fabrication of metal matrix nanocomposites (FMMNCs)

Fabrication of composites, nanocomposites, and porous and nonporous metal matrices are the same. The different metallic materials are obtained at the synthesizing stage *via* different procedures previously mentioned (Table 10). However, the final fabrication method, which can be

Table 7: Benefits and disadvantages of processes

Name of the process	Benefits	Drawbacks	Ref.
Sol–gel	– Not complex – Low temperature application – Adaptable – Multiple matrices achievable – Specific usage toward composite materials – No impurities on the final product – Formation of 3D metal-oxygen bonds	– The amount of porosity is low when compared to mixing strategy – Shrinkage is more often that affects the performance	[53–57]
Powder	– Not complex – Easy to operate	– Requires elevated working temperature – Energy intensive – High cost – Dispersion of particles is not very accurate – Formation of unwanted phases during production	[55,56]]
Polymer precursor	– Feasibility of producing better particles – More accurate/efficient scattering of particles within the matrix structure	– Production of inhomogeneous materials because of accumulation of fine products	[55,56,58]
Vapor phase	– Allows synthesis of ultrapurity nanoparticles – Size, shape, and internal structures are controllable – Reaction rate can be modified	– Does not produce a high yield, which makes this technique not suitable for industrialization	[67]
SHS	– High purity can be achieved – Energy efficient process – Can be used to produce high-quality metal matrices – Dense products – Short production rate – Not complex	– Energy-intensive process but consumption is high – Costly	[69,93]
Spray decomposition	– Homogeneous products – Elevated purity – Fast and easy process – No complex apparatus required – Low energy consumption – Suitable for magnetic metal oxide production processes	– Requires a lot of expensive solvents that increase the capital cost of the process – Mass production is challenging – Challenging to control the process parameters and variables that affect the outcome	[65,94]
Coprecipitation	– Simple application – Cheap reactants – Low poisonous waste products – Easy to control process parameters – Modifications on final homogeneity and particle surface is available – Low energy and temperature application – No organic solvent is required – Elevated quantity of magnetic products can be obtained by using this method	– Application on uncharged particles is not possible – Slow process and time consuming – Cannot be applied if there is a significant mismatch on the precipitation rates of the solvents – Distribution of the particles is not efficient, which makes coprecipitation prone to aggregation	[95–97]
Mechanochemical	– Suitable for nonstoichiometric halides synthesis at low temperatures – Eliminates the risks of high temperature applications such as thermal decomposition and high pressure	– Unwanted products can be produced which can lead to contamination of the final product. Oxidation is inevitable	[59,98,99]

Table 8: Distinctive manufacturing ways of CMNCs

Name of the process	Arrangement of the process	Technique	Ref.
Hot pressing	SiO_2/CNT	– Scattering of CNTs and silicon oxide glass powders into C_2H_5OH, mixing, and ultrasonic action	[55,56,100]
	SiC/CNT	– Drying off and hot-pressing sintering at pure nitrogen medium – Stirring and addition of SiC and CNTs together	
CVD or spray pyrolysis	Al_2O_3/CNT	– By anodizing CNTs into its holed walls, preparation of alumina matrix is achieved	[55,56,101,102]
(Highly used for porous ceramic manufacturing)		– CNTs grow toward hexagonal array of arranged vertical pores reaching the matrix surface from the substrate	
Catalytic decomposition	Al_2O_3 /CNT	– Utilization of C_2H_2 over Al_2O_3 powder soaked within the structure of the iron catalysts	[55,56,103]
Solvothermal process	Iron three oxide (Fe_3O_4)/CNT	– Scattering of CNTs in ethylenediamine utilizing ultrasonic process – Mixing of an iron three urea complex and heating in a Teflon-lined oven with an internal temperature kept steady at 200°C for 50 h – Cooling down to an optimal temperature	[55,56,104]

Table 9: The schematics of the manufacturing processes of CMNCs. The process schematics, which are not included are either chemical reactions or do not have any process units

Schematics of standard hot-pressing technique [89,105]

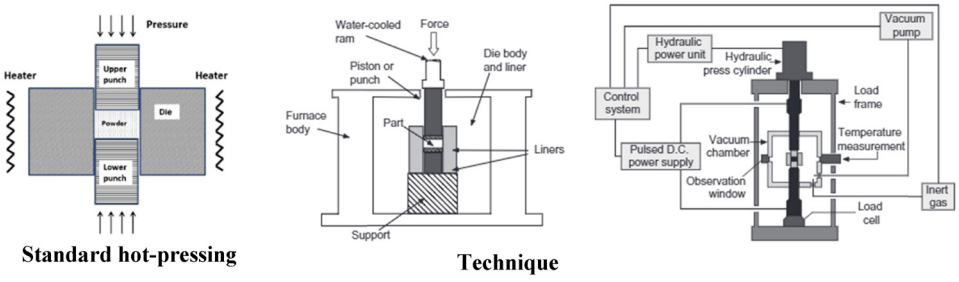

Schematic of CVD [106]

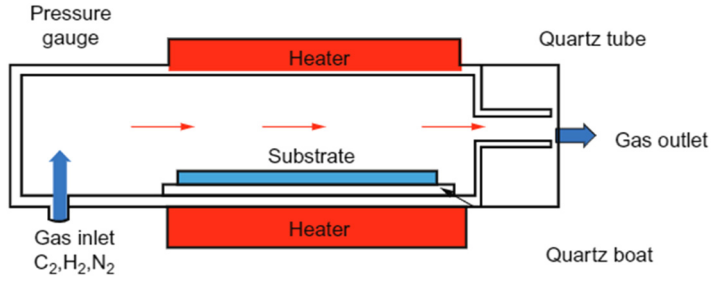

Schematic of catalytic decomposition method [107]

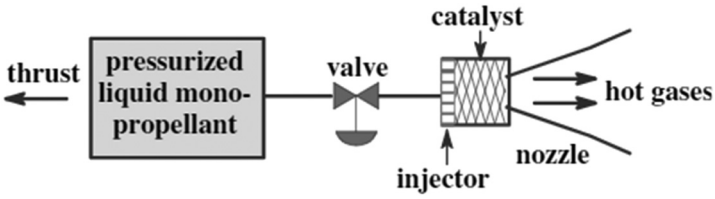

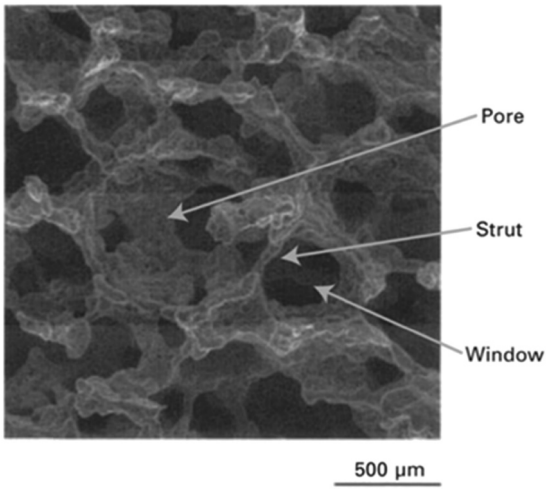

Figure 11: Closed-cell structured porous aluminium foam obtained *via* space holder method [120].

implemented to mass production is the same for every metallic composite branches. The following table illustrates the FMMNCs. A brief explanation of the process application as well as corresponding advantages and disadvantages is also depicted in Table 13.

In the previous section, the FMMNCs were given and explained in Table 13. Table 14 includes visual representation of the schematics with labels of the above-mentioned fabrication methods of MMNCs.

2.3 PMNCs

Fillers are the nanosized particles (nanofillers) used in PMNCs, which are categorized as 1D – linear, 2D – layered, and 3D powder. The link between polymer matrix and nanofiller at a molecular stage has an impact on the attraction between nanocomposites. As a result, supply of minor amount of nanofiller with dimensions smaller than hundred nanometers to matrix causes alteration on the overall composite material properties. Materialistic properties of PMNCs are elevated thermal stability, enhanced abrasion resistance and elevated barrier capacity (reduced gas permeability) [149]. To cite examples of PMNCs, thermoplastic/thermoset polymer/layered silicates, polyester/Tin oxide can be given [5]. Usage areas of PMNCs in daily life and industry are packaging, power tool housing, fuel and solar cells, and fuel tank [2].

2.3.1 Porous PMNCs

Porous polymers are becoming one of the most promising material group which are being started to utilize in almost every engineering sector. This research interest on such materials are due to their ability to own properties of both porous materials and polymers in a sole structure. Porous polymers have large surface area, exceptional physiochemical properties, ease of production and processing. Furthermore, porous polymers can be dissolved within a solvent and directly processed while maintaining the porous structure which is not possible to achieve in any other porous structures [150,151].

Figure 12 illustrates the scanning electron microscope image of macro porous polyurethane. The method utilized to produce this type of porous structure is known as gas foaming, which is the most popular technique. Various gaseous products obtained during chemical reactions can be used at some point in the manufacturing of the porous polymer which can be removed later to construct porous structure. In the production of macroporous polyurethane shown in Figure 12 the porous structure was obtained by removing the carbon dioxide molecules produced during the chemical reactions. This specific porous structure can be named as an open-cell structure, which is proven to be less dense and more flexible than the closed-cell structures [121,152]. Moreover, FGP polymer structures can be specifically designed to illustrate responsive properties with an additional ability to alter the pore structure relative to the engineering application. Porous state of the polymers can be altered between closed and open state when environmental exposure is the case. Additionally, since the structure of the porous polymers are organic and includes light components, the overall mass of the structure is significantly reduced, providing additional advantage of light-weighting [150,153,154]. Porous polymers are generally categorized by their size, physical shape, pore shape and dimension, spread of interconnectivity, and ultimate amount of porosity. The application which the porous polymer structure is supposed to be used is a deciding factor in terms of what kind of porous structure and mechanical properties of the polymer will have [155]. To effectively consider the porous polymer structure and respective structure's preparation and fabrication techniques, it is vital to divide the porous polymer structures into intersections. IUPAC has produced a template to classify the porous polymers relative to their pore size which is previously mentioned in the porous CMNCs section of this report. The union has agreed to separate porous structures into three distinct classes named as; microporous, macroporous and mesoporous. Note that, the porous structure of the polymer has a strong correlation with its manufacturing technique.

- *Microporous polymer structures* ($Ø_{microporous} > 2\,nm$)
  - The most important property of such polymers is high flexibility. This unique feature leads to efficient adsorption as well as cohesion applications. In

Table 10: Illustrating the processing methods for MMNCs

Process	System	Process	Procedure for MMNCs	Ref.
Spray pyrolysis	Iron/magnesium oxide, tungsten/copper	A thin film is positioned *via* spraying an occupied solution onto a high temperature surface. The reaction between the solution and the heated surface resulted in a chemical compound	– Preparation of the solvent to obtain liquid dissolution of the precursors – Obtaining of a "mist" from the previously prepared liquid dissolution utilized an ultrasonic atomizer – Utilization of a special gas bag to transport the mist into a previously heated compartment – Encouraging of the decomposition reaction to obtain relative oxides *via* vaporization of the droplets in the heated compartment and entrapping with a special filter – Production of metal oxides to achieve the respective metallic structures together with the selective reduction	[2,55,91,122]
Liquid metal infiltration	Lead/copper, lead/iron, tungsten/copper, niobium/copper, niobium/iron, aluminium–fullerene	This process is an alternative for squeeze casting. However, the infiltration operate fibers/particles *via* liquid metal is provided in the form of high-pressure inert gas, and the operation is performed in a vacuum atmosphere. A previously shaped template is located into a split metal die in the required shape of the part. Die and metal chamber is evacuated and high-pressure gas (*i.e.*, Ar) is applied to the melt compartment. Gas pushes the molten metal into the die to infiltrate the fiber. The pressure is kept steady until the solidification completes	– Integration of the nano-reinforcement particles to the metal matrix – Meltdown of the nano-reinforcements into the metal matrix by liquid infiltration *via* heat treatment – Additional heat treatment process lower than matrix melting temperature to ensure the consolidation and cancelation of internal excessive porosity	[2,55,122,123]
Rapid solidification	Aluminium/lead, aluminium/A/zirconium (A = silicon, copper, nickel) iron alloys	rapid solidification process process is a substitute to traditional casting methods for the processing of aluminium–copper alloys. The process includes the fast extraction of heat of a high-temperature molten metal to solidify. It is an elevated solidification rate process and can lead to noticeable variations	– Meltdown of metal components together (both reinforcements and the matrix) – Sufficiently high amount of heat is applied during the melting to ensure the miscibility is accomplished and the formed structure is homogeneous – Fast solidification of the melt. To cite an example, melt spinning can be conducted for solidification	[2,55,122,124]
Rapid solidification with ultrasonics	Aluminium/SiC	This new method includes the measurements of the interfaces during phase changes. The process is carried out during the fast solidification process. The operation requires echoes reflected from interfaces to track the	– Utilization of ultrasonics for mixing and to enhance the wetness among the metal matrix and reinforcing agents	[2,55,122,125]

(*Continued*)

Table 10: *Continued*

Process	System	Process	Procedure for MMNCs	Ref.
		solidification front. By this way, elimination of the temperature impact at the speed of sound in metals is possible		
High energy ball milling	Copper–Al_2O_3	Alternative name is mechanical alloying, which is a ball milling operation where a powder mixture located into a ball mill is exposed to energetic collisions sourced from balls. This process can lead to fine and good mechanical property materials	– Milling of the introduced reinforcing powders until the essential size is produced, that is, nanosized particles	[2,55,97,122]
CVD/PVD	Aluminium/molybdenum, copper/tungsten, copper/lead	CVD is an AM method, which is utilized to manufacture high quality and performance solids under vacuum conditions. The process includes chemical reactions occurring between a halide and an organometallic mixture to be placed and additional gases to obtain involatile thin solid films on substrates PVD is also an AM method. However, differing from the CVD where the material changes from a condensed form to a vapor form and again return back to a thin solid film condensed form	PVD: – Sputtering or evaporation of distinctive parts to obtain a vapor phase – Supersaturation of the vapor in a noble medium to encourage the condensation of the metal nanoparticles – Application of heat treatment in a noble medium to reinforce the nanocomposite CVD: – Gases are obtained via chemical reactions which are then solidified to required form.	[2,55,97,122,126]
Sol–gel, colloidal (chemical processes)	Silver/gold, iron/SiO_2, gold/iron/gold	Sol–gel: Method for adjusting and modifying the surfaces. The process includes hydrolysis of the precursor in either acidic or basic atmosphere followed by the polycondensation of the hydrolysis products creating a polymeric network where metal nanoparticles can be positioned Colloidal: Process developed to reinforce fine particles to eliminate heterogeneous agglomerates *via* either electrostatic repulsive forces or steric stabilization. Mentioned colloidal methods highly reduce large pores and lower the sintering temperature leading to a dense and fine nano/microstructure	Colloidal: – Metal pieces are utilized to lead the chemical reduction of salts in a solution – Reinforcement of the dry piece – To promote the selective oxide reduction and produce metal component, drying off and heating of the obtained solid are conducted in a reducing medium, that is, hydrogen medium Sol–gel: – Preparation of two distinctive micelles utilizing a mesoporous silica, which contains 0.1 mole chloroauric acid and 0.6 mole of sodium tetrahydridoborate – Mixing under the presence of UV light until the gold is reduced	[2,55,122,127,128]

(*Continued*)

Table 10: *Continued*

Process	System	Process	Procedure for MMNCs	Ref.
			For iron/gold containing nanocomposites: – Synthesis of the iron – Preparation of the secondary shell and dehumidification of the powders after second gold coating – Squeezing of the mixture to obtain the required material	

addition to this, empty spaces inside the polymer structure can promote effective interconnectivity [151].

- *Mesoporous polymer structures* ($2\,\text{nm} < Ø_{\text{mesoporous}} < 50\,\text{nm}$)
  - These specific porous polymers are manufactured *via* either soft or hard templating. The fundamental applications which mesoporous polymers are utilized are catalyst applications, synthesis of membranes, separation, and purification. Mesopolymers are proven to be used as organic semiconductors for osmosis and photocatalytic operations [151,156].
- *Macroporous polymer structures* ($Ø_{\text{macroporous}} > 50\,\text{nm}$)
  - Macropolymers are produced *via* cross-linking copolymerization of vinyl and divinyl monomers in a noble diluent. The diluent used during the mentioned reaction, which can be either linear polymer, nonsolvent or solvent, is the key factor in terms of determining the porous structure of the macro porous polymer. By being similar to microporous and mesoporous polymers, there is also a strong correlation between porous structure and the manufacturing method of macroporous polymers. To cite examples, freeze drying, porogenation, microemulsion formation, and gas blowing methods can be utilised to produce macroporous polymers. [150,151].

According to the Berro *et al.* [151], the most common preparation methods of porous polymers are; gas foaming, phase (immersion precipitation, chemically and thermally reaction driven phase separation) separation, small liquid drops templating (emulsion, bicontinuous micro emulsion and breath figures templating), colloidal crystal templating, templating *via* self-assembled structures, molecular imprinting and biotemplating utilizing natural biological templates. These methods are tabled in the following section. Production of pores on polymer structures, corresponding advantages and disadvantages are included in Table 15.

2.3.2 Processing of polymer matrix nanocomposites (PPMNCs)

The previous section explains the processing and preparation of porous PMNCs. Similarly, the following section is the categorization of the porous polymers. The main processing techniques are sol–gel, various polymerization methods, intercalation, and sacrificial template utilization. Table 16 summarizes the processing techniques of porous polymer nanocomposites with corresponding system arrangements and process procedures.

Table 11: Various processing method schematics of MMNCs. Processes for which schematics are not included are either chemical reactions or do not have any processing units

Schematic of spray pyrolysis with ultrasonics	[92]

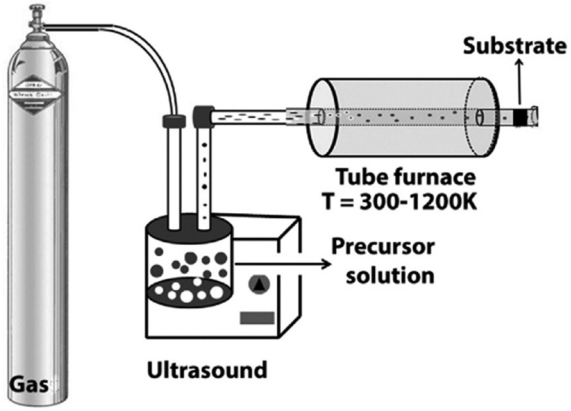

Schematic of liquid metal infiltration process	[129]

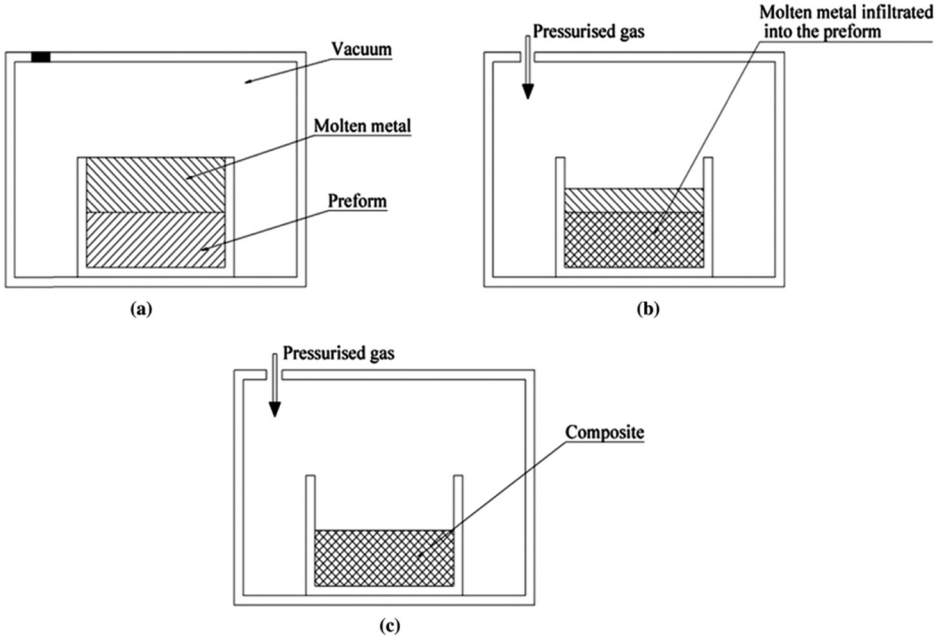

Schematic of rapid solidification with ultrasonics	[125]

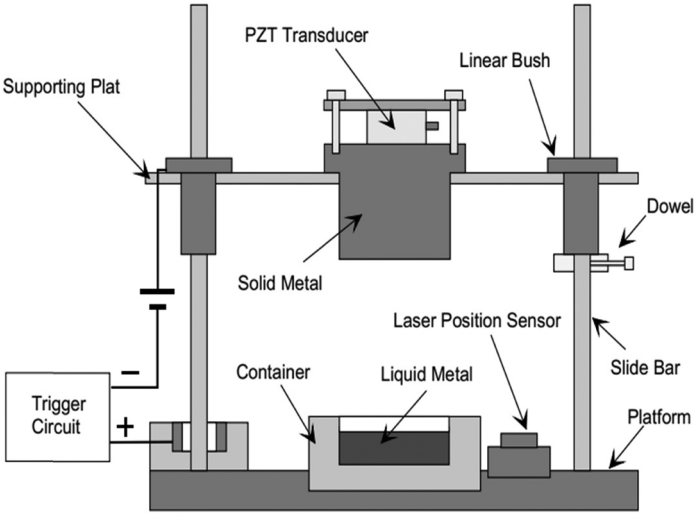

(*Continued*)

Table 11: *Continued*

Schematic of high energy ball milling	[130]

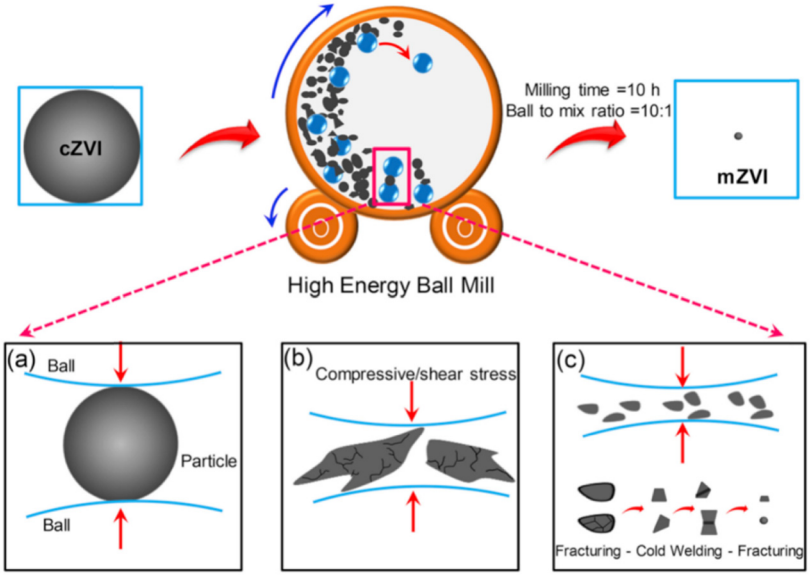

Schematic of PVD	[131]

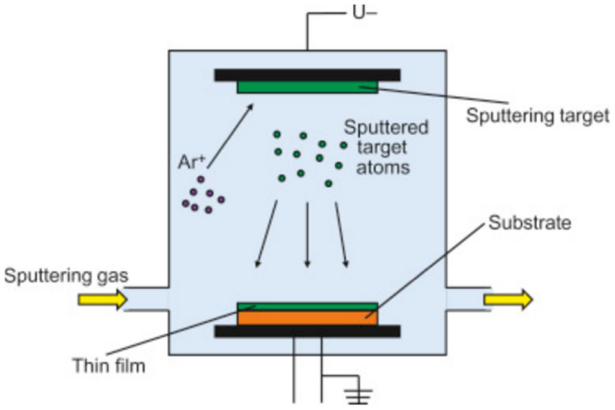

The previous section explains the processing techniques of PMNC systems. The following section summarizes the advantages and disadvantages about the mentioned PPMNCs in Table 17.

2.3.3 Fabrication of polymer matrix nanocomposites (FPMNCs)

Fabrication of polymeric, nanocomposites, and porous and nonporous ceramic matrices are the same. The different polymeric materials are obtained at the synthesizing stage with different procedures (Tables 15 and 16). However, the final fabrication method, which can be implemented to mass production is the same for every polymeric composite branches. Table 18 illustrates different FPMNCs. A brief explanation of the process is available together with the relative advantages and disadvantages of every manufacturing process.

The previous section explains the main fabrication methods of PMNCs with brief explanation as well as advantages and disadvantages. The next section is the visuals of the above-mentioned manufacturing processes utilized during the manufacturing of PMNCs. Table 19 depicts the schematics of the processes explained previously in Table 18.

Table 12: MMNC processing techniques along with the relative advantages and disadvantages

Process	Benefits	Drawbacks	Ref.
Spray pyrolysis	– Efficient production of very good quality, fine, shaped, and homogeneous particles – Cost-effective method – Does not need high-quality reagents – Surfaces, morphologies and shapes can be efficiently controlled by modifying operation conditions and supplies	– Not a scaled-up method (low product levels) – Oxidation of sulfides can be a major issue in an air atmosphere – The growth temperature is challenging to modify – Expensive when large batches required to be produced	[2,55,123]
Liquid metal infiltration	– Complex shaped part production is available – Lower pressure levels – Lab-scale production and scaled-up industrial productions are available – Minimized contact time between the matrix and reinforcements	– Uncontrollable porous structures – Not very efficient mechanical properties, that is, low wear resistance – Bonds between the particles are not strong	[55,122,123]
Rapid solidification	– Extension of the solid solubility – Production of metastable crystalline phases – No microsegregation during solidification – Good cellular structure – Enhanced grain size and shape – Easy and efficient technique	– Solely operated for metal nanocomposites – Agglomeration and inhomogeneous dispersion of grains	[55,122,124]
Rapid solidification with ultrasonics	– Efficient dispersion without agglomeration – New technique	Not specified	[55,122]
High energy ball milling	– Relatively inexpensive – Ease of scaling up to produce large volumes – Homogeneous mixing of materials – Uniform scattering of reinforcement particles	– Challenging to classify with respect to particle size – Causes surface contamination	[55,122,132,133]
CVD/PVD	CVD: – High-purity products with uniform grains can be produced – Capable of producing high-density and pure materials – Uniform depositions – Good adhesion and reproducibility PVD: – Improved mechanical and material properties – Compatible with all inorganics and most organics – Eco-friendly process	– Costly and complex process – Relatively low yield – Costly and complex – Challenging to coat complex structured shapes – Relatively low yield	[55,122,134]
Sol–gel, colloidal (chemical processes)	Sol–gel: – Efficient, effective, and versatile – High-purity final products – Low-temperature application – Produces large and stable surfaces Colloidal: – Simple process – High chemical homogeneity	– High porosity – Reduced wear resistance – Low internal bonding strength – Controlling porosity is challenging – High permeability	[2,55,127]

2.4 Applications of porous nanocomposites in various engineering sectors

The application of porous nanocomposites offers improved mechanical and material properties of the engineering assemblies. Distinctive engineering sectors including biomedical, electrical and electronics, aerospace, marine, mechanical, and energy storage are greatly demanding constant development and innovation on the material usage in many engineering applications for improved efficiency and longer service life. To cite, Pinkert *et al.* [186] studied the spatial separation of the metal

Table 13: The fabrication methods of the MMNCs along with the advantages and disadvantages

Process name	Application	Advantages	Disadvantages	Ref.
Stir-casting	Stirring mechanism is integrated into the molten metal and constant stirring is performed to ensure a steady dispersion of nanoparticles within the molten matrix	– Versatile – Cheap – Not complex – Very compatible with aluminium and magnesium matrices	– Cluster can be formed between nanoparticles because of high surface area, which can lead to elevated van der Waals forces among nanoparticles – High porosity as a result of air bubbles trapped in the mixture due to stirring – Wetness of the solid particles cannot be controlled within the molten matrix	[135–137]
Disintegrated melt deposition (DMD)	Molten composite called "slurry" is produced similar to stir casting process. The obtained slurry is transported through a pouring nozzle where high temperature (up to 1,200 K) noble gas is present (*i.e.*, Ar). After the pouring operation is finalized, the slurry is transferred onto metal substrate. The final form of the nanocomposite is an ingot, which then can be reformed to a required final shape *via* hot extruding process	– Highly compatible with magnesium metal – Eliminates excessive oxides and waste metals	– Energy-intensive process – High amount of heating is required for elevated noble gas temperature – High cost	[137–140]
Semisolid casting (SSC)	Highly accurate die casting method. The nanocomposite material is transported into a mold hole in a semiliquid/semisolid state, and the casting process takes place at mold cavity compartment	– Lowered energy consumption compared to other methods – No postprocessing is required – Finish quality of the part is very good – Porosity levels in SSC structure is negligible	– Producing materials with complex shapes (*i.e.*, circular, spherical) is challenging	[137,141]
Power metallurgy (PM)	This technique uses solid materials to cast. The solid reinforcement and matrix materials (mainly in powder form) are blended until a required composition is achieved. The process is followed by a squeezing process to obtain a "compaction." The casting process is terminated by sintering *via* microwave energy. To ensure the quality of the product is decent, sometimes equal channel angular pressing or extrusion processes can be applied at high temperatures	– Capable of producing complex shapes (*i.e.*, near net shaped) – Adjusting the volume of nano-reinforcing units within the metal matrix is possible with this method – Mass production and elevated batch volumes is achievable	– Equipment of PM are costly only viable in the case of mass production – Raw material cost is high – Sometimes density of identical parts can vary due to uneven compression – Mechanical properties of PM parts are not very good compared to machined parts	[137,142]
Friction stir processing (FSP)	FSP process is very similar to friction stir welding, which is very common in many manufacturing sectors to integrate nanomaterials into a metallic matrix to obtain bulk or surface nanocomposites. A grove of required metal matrix is filled with nano-reinforcements. A rotating pin-less tool attached to the substrate is used to close the groove trapping	– New technology – Efficient process – Energy consumption is not very high – Quality process – Very compatible with magnesium and aluminium components, which leads to enhanced mechanical properties	– Surface of the final product is not quality. – Distribution of nano-reinforcements is not uniform due to uneven stirring	[137,143,144]

(*Continued*)

Table 13: *Continued*

Process name	Application	Advantages	Disadvantages	Ref.
	the nanoparticles inside. A pinned stirrer spread the particles within the unit to produce good mixing ratio			
Accumulative roll bonding (ARB)	ARB is composed of many plastic deformations created by a rotating mechanism on the surface of stacked metal sheets. ARB steps are cleaning of the metallic sheets by wire brushing to remove any contaminants. Positioning two metallic sheets on top of each other. Roll bonding of the metallic sheets until a minimum of 50% thickness reduction is observed. Separation of the roll-bonded components into smaller sections	– Suitable for continuous production – Distinctive shapes can be obtained from bulk metals such as, plates, sheets, and bars – High-temperature bonding eliminates accumulated strain, which leads to superior process	– Material properties, especially plastic strain is compromised as the process itself is a deformation process – High temperature is costly to achieve	[137,145]

hydroxide nanoparticles within the porous carbon matrix. Efficient distribution of the nanoparticles within the functionalized porous carbon network revealed improved energy density levels, which leads to an efficient supercapacitor utilization in electronics. Moreover, porous magnetic nanocomposites used in biomedical engineering showed enhanced mechanical properties especially higher tensile strength. scanning electron microscope (SEM) images illustrated improved internal connection between macroporous and microporous structures, which is the reason of improved strength. Magnetic Fe_3O_4 nanoparticles are utilised for abovementioned biomedical engineering applications due to its reasonable water absorption properties as well as healthy antimicrobial possessions. [187]. To sum up, different nanocomposite assemblies are used in different engineering sectors. To cite an example, porous MMNCs are highly preferred in medical, aeronautics, marine, transportation (land and air transport), and military protection applications [188]. Moreover, porous PMNCs are mainly used in food packaging, coating, adhesion, drug delivery, electric, and electronic applications [189]. However, porous CMNCs are mainly utilized in industrial, civil, and energy absorbing applications [190]. The differences among the application areas of three nanocomposites originates from the variations between morphological, atomical, and bonding structures. Table 20 has been added to illustrate distinctive porous nanocomposite materials along with their relative engineering sector.

3 Numerical, mathematical, and computational modeling review

A research conducted by Ansari *et al.* [210] studied geometrically nonlinear static bending of FG-GPLRC porous plates. Four distinctive porous dispersion plan and patterns were selected, and material characteristics were deduced by using closed-cell Gaussian random field (GRF) scene, the Halpin–Tsai micromechanical model, and the rule of mixture [15,18]. To process the data on computer, authors used virtual work principle and higher-order shear deformation theory (HSDT) derivations in matrix form. Variational differential quadrature (VDQ) and finite elemental methods (VDQ–finite element modeling [FEM]) numerical approach was used. The problem domain was divided into finite elements and VDQ selection method was exploited for every finite element model. Authors used the mentioned procedure to investigate the impact of porosity and GPL dispersions. Resulting matrix equations were solved with the help of the pseudo arc-length continuation algorithm.

Table 14: Various fabrication methods of MMNCs

Schematics of stir-casting	[137]

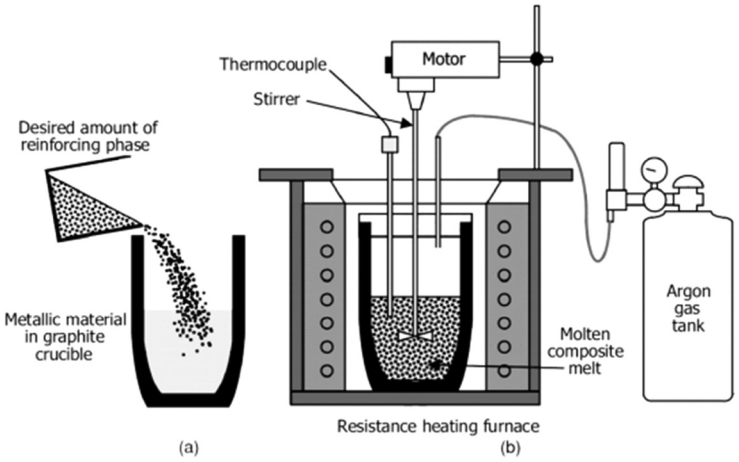

Schematic of disintegrated melt deposition	[146]

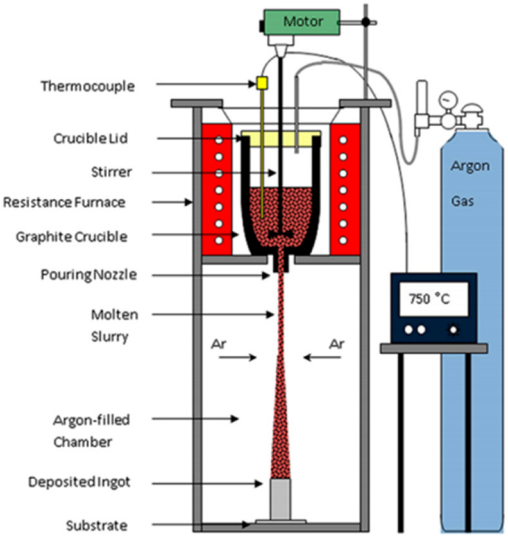

Schematic of powder metallurgy	[147]

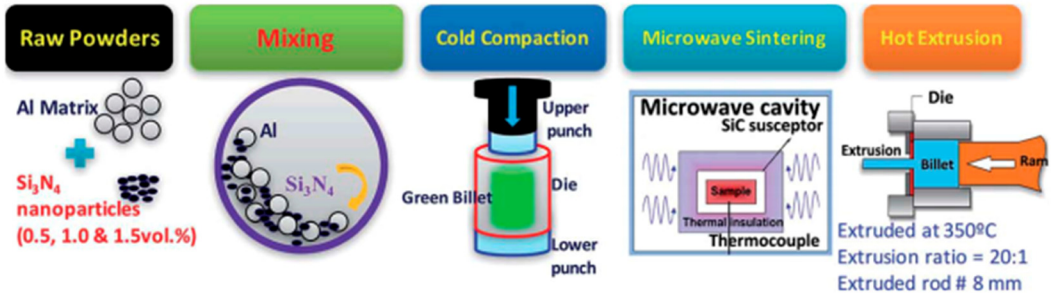

(*Continued*)

Table 14: *Continued*

Schematic of FSP	[148]

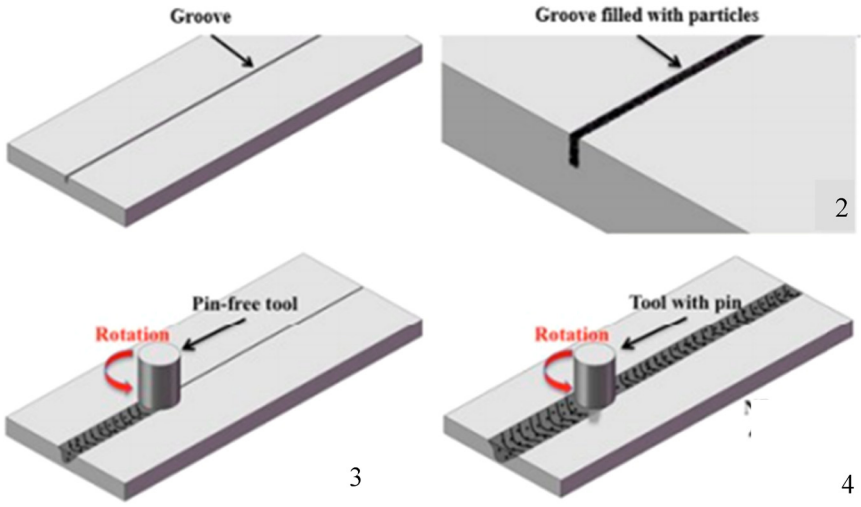

FSP grooving process, (1) filling of the powder material, (2) pinless FSP, (3) pinned FSP (4) [148].

Schematic of ARB	[137]

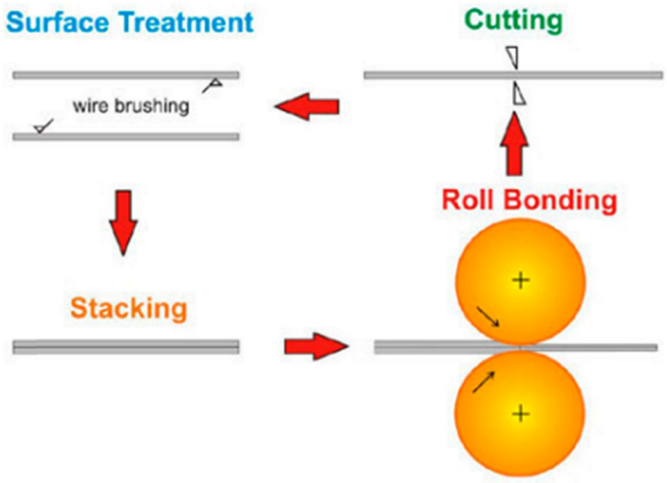

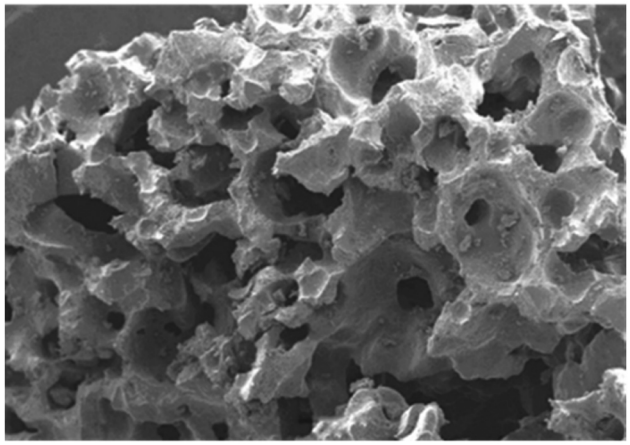

Figure 12: SEM image of polyurethane [152].

This study highlighted the tendency of VDQ–FEM propose efficiency for solving problems. Another study carried out by Yas and Rahimi [15] examined the variation of thermal buckling of FGP nanocomposite beams under distinctive temperatures by using generalized differential quadrature method (GDQM). Different nanofillers, scattering patterns, and porosity allocations were studied. GRF was used together with closed-cellular solids to obtain Poisson's ratio and correlation among porosity coefficient and mass density. Halpin–Tsai micromechanics modeling was utilized to determine elastic modulus of the nanocomposite. Arshied *et al.* [211] utilized the GRF model method for closed-cell cellular

Table 15: Indicating methods for processing and preparing porous polymers

Technique	Production method of pores		Advantages	Disadvantages	Ref.
Direct templating	Space obtained *via* elimination of the templates. Mainly chosen for soft materials		– Easy – The manipulation of the meso/macroporous structure is possible – Functional grading is achievable	– Requires sacrificial templates – Complex and costly for scaled up production – Not very efficient pore production – Cannot be utilized effectively for hard materials	[150,157]
Block-copolymer self-assembly	Space obtained *via* removal of sacrificial component, morphology regeneration, and vesiculation Two different polymers bonded covalently to self assemble to form a specific structure in nanoscale-customized pore size		– Customized pore structure and arrangement – Suitable for complex structures such as stimuli responsive assemblies	– Not a very effective method for mass production – Expensive – Absence of micro or nanopores	[150,158]
Direct synthesis	Microporous	Links between monomers are hyper-cross linkable	– High surface area of this structure enables permanent porosity – Pore structure can be customized by customizing the monomer structure used in the porous assembly	– There is only one way that the monomers for this process can be produced – Expensive process and raw materials – Control of the resultant pore structure is challenging – Low reaction rate – Low yield	[150,159]
	Mesoporous/macroporous	*Via* phase generation	– Ease of control of the process and the resultant structure	– Microporous structures are complex to achieve *via* this method – Low reaction rate – Low yield	[150,159]
High internal phase emulsion polymerization	Space obtained *via* changing of the internal phase		– Elevated porosity levels (75–95%) – Exceptional void and frame structure are achievable	– Low surface area – Weak mechanical properties	[150]
Interfacial polymerization (IP)	IP takes place between two nonmiscible solutions causing spaces to occur due to the removal of the micelle		– Very compatible in terms of synthesizing nanocapsules	– Pore structure control is challenging	[150,160]
Breath figures	Water droplets bombarded from a cold region to warm surface led to the production of micro/nanopores *via* condensation of water droplets from the templates		– Simple – Honeycomb structure can be obtained	– Producing nanopores (<100 nm) is challenging	[150,161]

Table 16: The processing techniques of PMNCs

Name	System	Process	Ref.
Sol–gel	Polyimide/silicon dioxide, polyimide/silica, polyethylacrylate/silicon dioxide, polycarbonate silicon dioxide, polyimide	This process further divides into two which are metal alkoxides hydrolysis and polycondensation of the hydrolyzed product. Halides, metal alkoxides, esters, and many more various organics can be used to produce inorganic metal oxides	[55,162]
(1) Mixing/(2) *in situ* polymerization	Polyvinyl alcohol (PVA)/silver	Mixing: This synthesis includes mechanical mixing of a polymer solution and effectively distributed nanoparticle solution	[162]
	Polymethyl methacrylate/Pd polyester/ titanium dioxide polyethylene terephthalate/calcium carbonate epoxy vinyl ester/Fe_3O_4 Epoxy vinyl ester/gamma-Fe_3O_4 Poly acrylic acid/silver, poly acrylic acid/nickel poly acrylic acid/copper silver nitrate Silver sulfate Copper sulfate	*In situ* polymerization: Requires monomers and initiators. With the help pf clays, polymerization occurs. With the growth of the polymeric chains, clays start to spread and polymer chains fill the created interlayer space leading to a polymeric-clay structure	
Template synthesis	Hectorite with polyvinylpyrrolidone Hydroxypropyl methylcellulose Peroxyacetyl nitrate Poly diallyl dimethylammonium chloride Polyaniline	By utilizing this process can obtain exfoliated nanocomposites. Inorganic material synthesized in a polymer matrix (PM). PM favors the growth of inorganic host crystals and captures them within the layers	[162,163]
Melt intercalation	Montmorillonate with positronium Polyethylene oxide (PEO) Poly propylene Polyvinylpyrrolidone Clay-polyvinyl phenol	Melting high-molecular weight polymer at elevated temperatures. Nanofillers are added to the polymer melts under shear. This is a solvent-free process, that is, no chemical reaction is required	[162–164]
In situ intercalative polymerization	Montmorillonate with N6/ polycaprolactone (PCL) Polymethyl methacrylate Poly urethane Epoxy	The process utilizes monomers, which includes layered particles. Polymerization of the monomers is started. Structures obtained by this method is highly exfoliated due to the allocation of monomers at both inside and outside of the interlayers	[162–164]
Intercalation/polymer from solution	Clay with PCL PLA High-density polyethylene PEO PVA Polyvinyl pyrolidone	This process uses distributed nanofillers in a solvent and an additional soluble polymer. Process includes the absorption of the polymer by the delaminated sheets with a simultaneous evaporation of the solvent. After all the solvent has been evaporated, the sheet formation is adjusted to trap the polymer chains between the layers. Thus, multilayered structure can be achieved by this method	[162,163]

solids for the porous matrix characteristics and effective features of porous nanocomposite was obtained by Halpin–Tsai along with extended rule of mixture micromechanics model. Shear deformation impacts were considered by using the first-order shear deformation theory (FSDT). Energy method was used to derive equations and solved by generalized differential quadrature (GDQ).

To understand the thermoelastic manners of sandwich plates with porous polymeric core and CNT clusters/polymer nanocomposites, Safaei *et al.* [17] used total energy function along with mesh-free strategy together with two-plate theories to deduce the leading thermoelastic equations. To monitor the temperature dependency of the CNT clusters/polymer nanocomposite, Eshelby–Mori–Tanaka's method was operated. Yang *et al.* [212] utilized FSDT to consider the transverse shear strain and Chebyshev–Ritz approach to discretize the displacement fields. Leading equations were extracted and then solved to deduce critical uniaxial,

Table 17: The advantages and disadvantages of PMNC processing methods

Name	Benefits	Drawbacks	Ref.
Sol–gel	– Not complex – Low operation temperature – Versatile – Efficient chemical homogeneity – Stoichiometry control – Elevated purity (clean/pure samples) – Successful in terms of producing inorganic–organic hybrids	– High amount of shrinkage – Relatively reduced amount of voids	[55,162]
Template synthesis	– Suitable for batch production – Not complex	– Exclusively compatible with water soluble polymers – Contamination	[55,162]
Melt intercalation	– Cheap – Simple procedure – Eco-friendly – Can be integrated to industrial manufacturing (suitable for batch production)	– Applicable together with the use of polyolefins, which are not environmentally friendly products	[55,162]
In situ intercalative polymerization	– Not complex – Controllable dispersion of nanoparticles within the polymer precursors	– Not suitable for many applications – Challenging to regulate intragallery polymerization	[55,162]
Intercalation/polymer from solution	– Homogeneous reactant polymers – Reduced polarity polymer reactants	– Expensive – High solvent consumption	[55,162]

biaxial, and shear-buckling stresses, as well as the natural frequency of the plates with distinctive porosity and GPL dispersions. Moreover, to scrutinize material properties of graphene-reinforced nanocomposites, similarly, Liu *et al.* [18] used Halpin–Tsai and rule of mixtures. In addition, free vibration and bending equations of nanocomposite were derived with the help of 3-D elasticity theory together with the state space method. Jalal *et al.* [213] proposed usage of big data approach for an efficient design of composite structures, which mainly considered functionally graded carbon nanotube-reinforced nanocomposites. The materialistic features of the nanocomposites were deduced *via* Eshelby–Mori–Tanaka method. Followingly, researchers compared two methods of using big data approach, which are mesh-free method and optimized neural network (ONN). Robust mesh-free technique was utilized to extract vibrational frequencies, impact of CNT alignment and aggregation. Six parameters (geometry dimensions, composite core, nanocomposite layer, volume fraction of CNTs and clusters, volume fraction of changing exponent) included a total of 15,625 data sets, which are followingly analyzed by ONN. ONN results were found to be very consistent and confirmed the suitability of ONN's usage for enormous data analyzing. Furthermore, utilization of ONN is nearly a thousand times faster relative to mesh-free method with negligible amount of simulation error [214]. Yaacoubi *et al.* [215] studied loading distributions and shifting in sandwich plates, which reinforced with functionally graded nanocomposite face sheets was tested by FSDT built on mesh-free strategy. The assembly was treated as Winkler–Pasternak elastic model, and the nanocomposite was consolidated with three distinctive CNTs. Molecular dynamics (MD) study at nanoscale and Halpin–Tsai were utilized to deduce the elastic constants of the assembly. The adjustment of boundary conditions was vital. This was accomplished by utilizing moving least squares (MLSs) to approximate the displacement field and the transformation technique.

Temperature plays an important role on the nonlinear free vibration of edge-cracked graphene nanoplatelet (GNP)-reinforced composite laminated beams [216]. Supposing GNPs fillers were dispersed randomly and thermal field was distributed uniformly, material properties of the GPLRNC was found *via* micromechanical models. Loading and intensity coefficients were deduced *via* FEM. Karman-type geometric nonlinearity with respect to FSDT was used to derive crack motion equations. The bending stiffness of the cracked section was modeled *via* massless rotational spring model, and finally, differential quadrature technique was utilized to extract both linear and nonlinear natural frequencies of the ruptured GPLRNC beams

Table 18: The manufacturing methods utilized to produce PMNCs as well as relative advantages and disadvantages

Manufacturing method	Description	Advantages	Disadvantages	Ref.
Wet lay-up	Required composite resin to be transported into a mold and treated for consolidation. Can be carried out either *via* spray pistol or manually by hand	– Simple – Low cost	– Poor final mechanical property products – Nonuniform distribution of the resin – Excessive voids on the final product	[164]
Pultrusion	Nanofibers are pulled by a high-temperature dye. During the pulling, a steady pressure is applied to melt the resin and to deposit the melt into the fibrous reinforcing agent	– Cheap – Continuous – Fast – Efficient alignment of fibers can be regulated *via* optimization of the manufacturing parameters	– Process wastes can accumulate at the edges and can cause disorders (unexpected final product shapes) – Excessive void production – Constant cross section is hard to obtain	[164,165]
Resin transfer molding (RTM)	RTM is a closed molding application where polymer matrix is deposited over preplaced reinforcing fibers, which is followingly placed onto a mold	– Cheap – Compatible with high batch production	– Requires advanced equipment for tooling and design (*i.e.*, expensive) – Complex application – Complex parts are challenging to obtain – High resin viscosity can block the flow	[164,166,167]
Vacuum-assisted RTM	Integrated RTM process where vacuum is utilized to improve resin flow and to decrease void formation. Layered composites are insulated with a plastic material. Resin is directed to the wrapped parts to fill the voids between the composite layers	– Reduced resin flow blockage – Low-cost application for high-volume production – Huge and complex parts can be produced – Enhanced final surface and better mechanical property products – High fiber volume fraction	– Possible dryness at certain places – Nonuniform dispersion of resin is possible for some specific shapes	[164,168,169]
Filament winding	Resin impregnated fibers are wrapped over a mandrel at distinctive angles to form a piece	– Complex parts can be produced – Viscosity problems are eliminated – Cost effective	– Limited to the shape of the part, only certain structured shapes can be produced – Crossovers points can decrease the quality of the final product	[164]
Fiber placement technology	Prepreg plies can be located automatically and quickly with good geometry in a short period of time	– Automated – Fast – Accurate	– Size of the fiber used affects the performance of the process, that is, large geometry fibers can increase the production time	[164,170]
Autoclave processing	Open molding process where molded piece is enhanced with the help of the vacuum, heat, pressure, and inert gases. The molded piece is then transported in a plastic bag and the trapped air is discharged *via* an exhaust. This eliminates air inclusions and volatiles. Followingly, heat, gases, and pressure within the autoclave cures and consolidates the material	– Widely used industrial method – Complex and high-quality parts can be produced – Both thermosets and thermoplastics can be manufactured with reduced thickness and reduced porosity – Homogeneous parts	– Highly expensive – Elevated capitalized cost	[164,171]

(*Continued*)

Table 18: *Continued*

Manufacturing method	Description	Advantages	Disadvantages	Ref.
Resin film infusion (RFI)	Similar to an RTM process. A thin sheet of solid resin is placed into the mold and preform is placed on top of the resin sheet with the presence of heat and pressure	– Cheap molds – High fiber volume fractions	– Labor-intensive process	[172]

[25,217–220]. Nguyen *et al.* [39] proposed an effective numerical method to investigate and regulate geometrically nonlinear responses of the FGP plates consolidated with GPLs integrated with piezoelectric segments. The methodology was the utilization of iso geometric analysis (IGA) based on the Bezier extraction and the C zero type HSDT (C^0 – HSDT). By using the Bezier extraction, the original nonuniform rational B-Spline (NURBS) control meshes were converted into the Bezier elements, which lead to receive the standard numerical process such as the finite element method (FEM). The mechanical shift field was estimated based on the C^0 – HSDT, whereas the electric potential was supposed to be the function of the thickness of every single piezoelectric sublayer. The FG plate contains the inner pores and GPLs distributed in the matrix either uniformly or nonuniformly rendering distinctive patterns along the thickness of the plate. Moreover, to manipulate dynamic feedbacks, two piezoelectric layers were attached to the top and the bottom faces of the plate. The geometrically nonlinear equations were solved by the Newton–Raphson iterative technique and the Newmark's time integration scheme. Furthermore, a steady shift and velocity response control methods were implemented to effectively monitor both nonlinear dynamic and static feedbacks of the plate. With the help of this strategy, structural damping, based upon a closed loop control with piezoelectric instruments, was scrutinized.

Set of tables below has been included to categorize various modeling of nanocomposites, which have been extensively discussed above. Distinctive categorization has been done for different nanocomposite types. To cite an example, Table 21 illustrates the modeling parameter nanocomposite beams. Similarly, consequent Tables 22 and 23 illustrate modeling parameters for nanocomposite plates and for nanocomposite shells, respectively.

Categorization of nanocomposite in terms of analysis model, mathematical model, numerical approach, equations derivation method, and computational algorithm (if used in the study). Table 22 depicts the modeling classification of nanocomposites plates.

Grouping of nanocomposites in terms of analysis model, mathematical model, numerical approach, equations derivation method, and computational algorithm (if used in the study). Table 23 depicts the modeling classification of nanocomposites shells.

Table 24 includes the summary of the key assumptions and the main distinctions of mechanical models, which have been previously discussed in Tables 21–23 in detail.

Table 19: The schematics of the various FPMNCs

Schematics distinctive wet lay-up methods	[173,174]
Hand lay-up 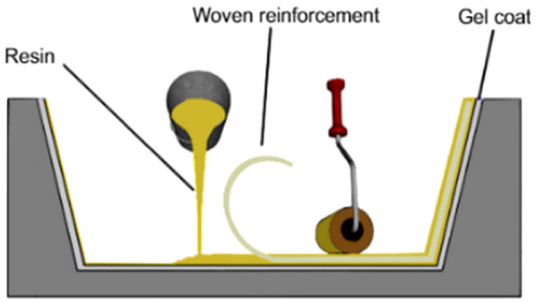	Spray lay-up 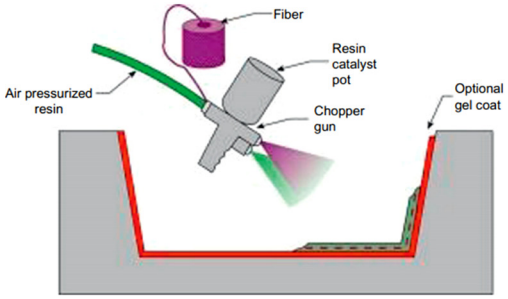
Schematics of pultrusion	[175–177]
Resin injection pultrusion 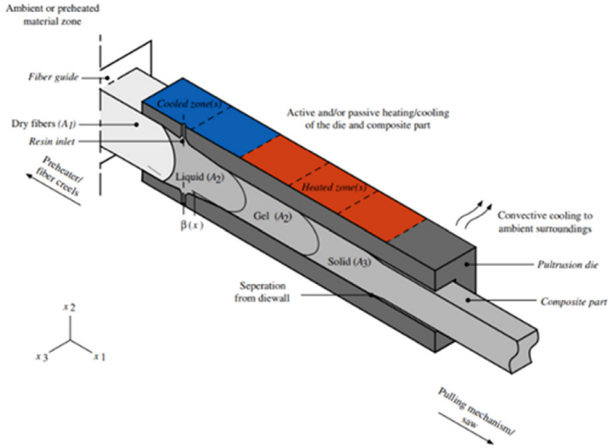	Conventional pultrusion process 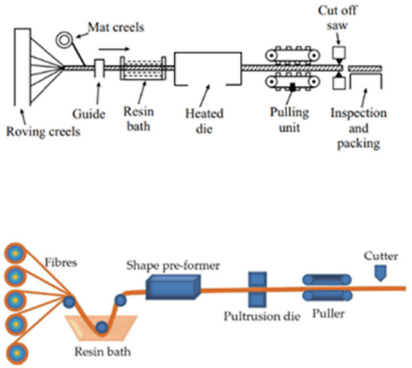 Compartments of resin infusion-pultrusion: A_1: Resin flow front (resin enters the pultrusion unit from this point) A_2: Middle section (resin is at both liquid and gel states in this compartment) A_3: Solidification zone (where temperature decreases and resin solidifies)

(*Continued*)

Table 19: *Continued*

Schematic of RTM	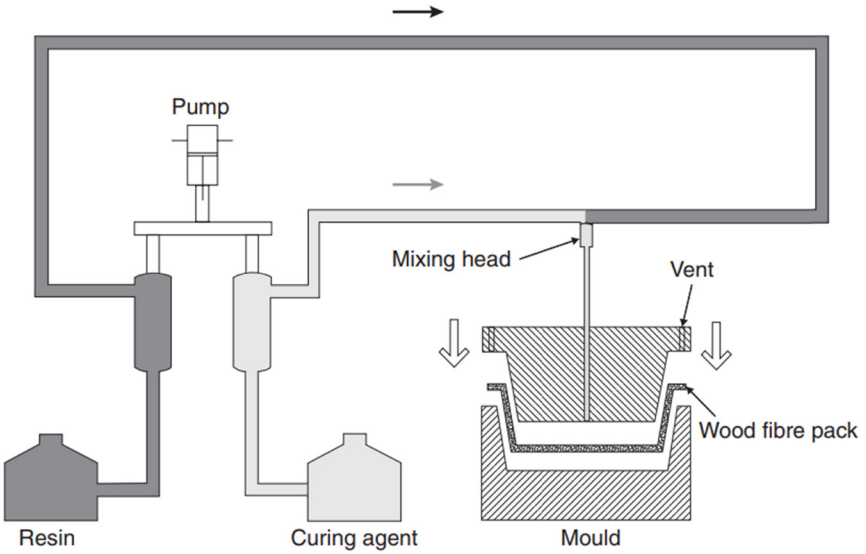	[178]
Schematic of vacuum-assisted RTM	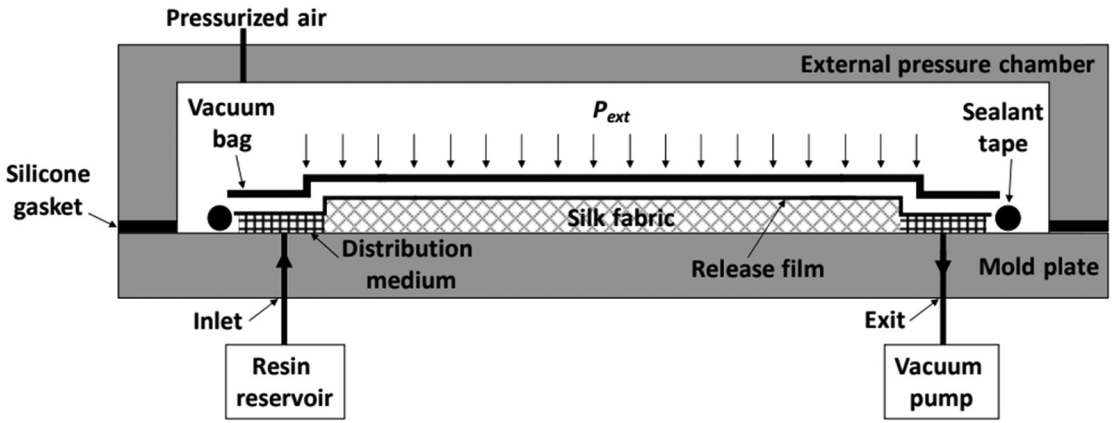	[179]

(*Continued*)

Table 19: *Continued*

Schematics of filament winding process	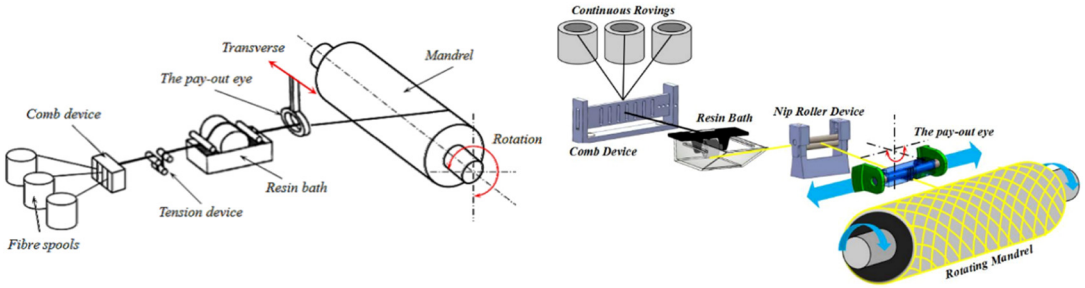	[180,181]
Schematics of fiber placement technology	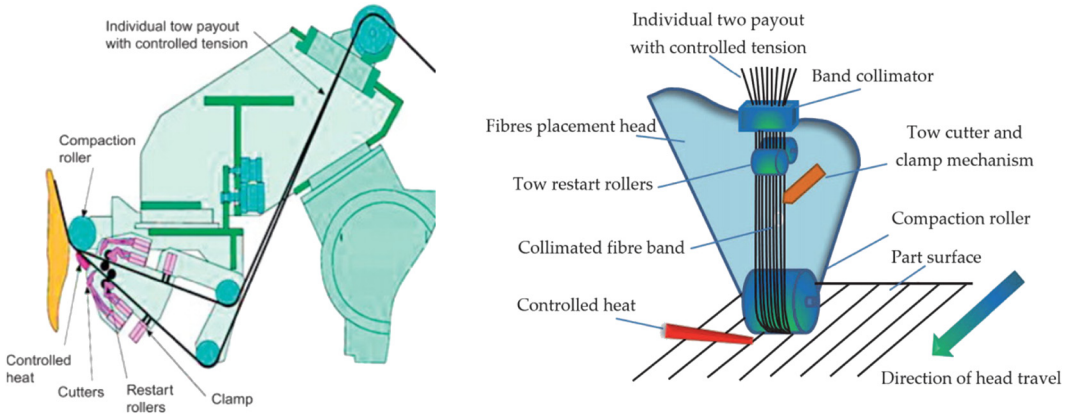	[177,182]

(*Continued*)

Table 19: *Continued*

Schematic of autoclave processing	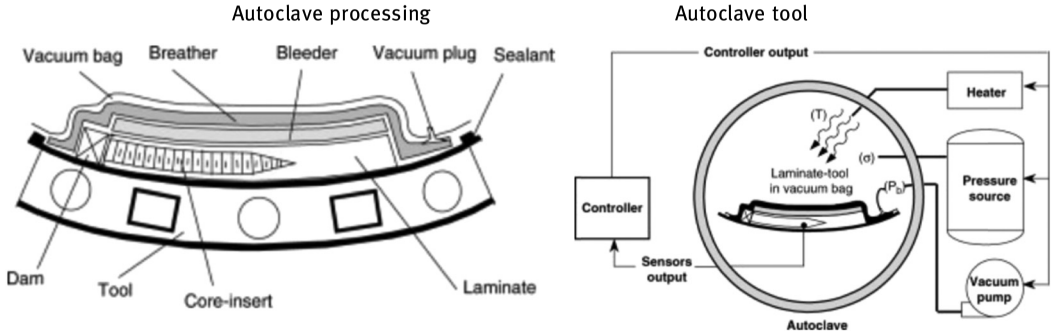	[183]
Schematic of RFI	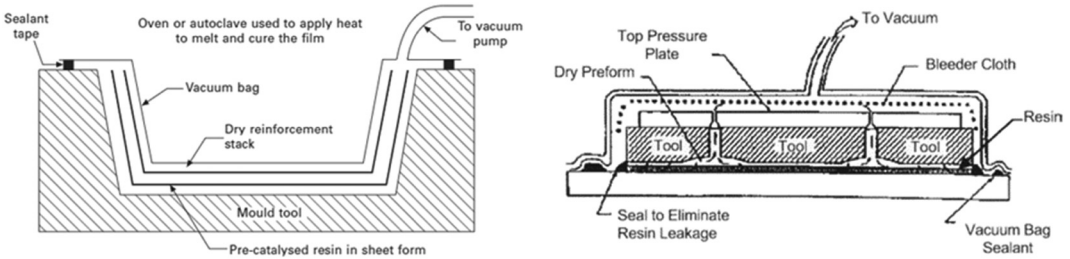	[184,185]

Table 20: Various nanocomposites and their respective usage in the engineering sector

Nanocomposite	Applications in engineering	Ref.
C/MoS_2	Novel electrode material for supercapacitors	[191]
Ag/carrageenan–gelatine hybrid hydrogel	Biological applications including tissue engineering, regenerative medicine, antimicrobial, anticancer, and drug delivery	[192]
Fluoroalkyl end-capped oligomeric	Biomedical, pharmaceutical, coatings, electronics, optics, and diagnosis	[193]
Polyhedral oligomeric silsesquioxanes (POSS)-based polyamide	Thermosets, thermoplastics, drug delivery, solid polymer electrolytes, membrane applications (desalination, gas separation), food packaging, and automobile (fuel tanks)	[194]
POSS-based biocompounds	Dental applications, drug delivery, and tissue engineering	[194]
Organo/rubber/clay nanocomposites	Automotive, flame retardant, and lightweight	[195]
Polymer/silica/colloidal	Gas barrier coatings, catalysts, and chromatography	[18]
Graphene based	Energy (batteries, fuel cells, PVs), environmental	[196]
ZnO	Domestic and industrial	[197]
Polymer (PMNC)	Solar cells, sensors, and conductance thin films	[197]
Layered double hydroxide sheets	Cosmetic (allowable permeable membrane production)	[198]
Polymer pencil (porous graphite material)	Electrode utilization, electrochemical analysis of materials	[199]
Porous graphene nickel oxide	Supercapacitors, energy storage, and regenerative systems	[200]
Porous ZnO/C	Several energy storage (fuel cells) and environmental (used as catalysts in many vital reactions such as hydrogen evolution reaction during water-splitting process) applications	[201]
Carbon nanofiber polydimethysiloxane (CNF/PDMS)	Sensing applications. Can be utilized as piezoresistive sensors in numerous engineering sectors	[202]
Carbon coated MnO	Utilized as anode in electrochemical applications	[203]
Porous silica–graphene	Environmental-aimed applications. Removal of contaminants such as oil, heavy metal, organic solvent, and dyes from water	[204]
Honeycomb-like porous zinc carbodiimide-based nanocomposites	Electronic applications. Used to manufacture asymmetric supercapacitor cells	[205]
High porosity-reduced graphene oxide/$NiCo_2S_4$	Electrode materials for electrochemical applications (reduced graphene oxide being anode active and $NiCo_2S_4$ being cathode active material)	[206]
Multifunctional Fe_3O_4/N_2 doped-porous carbon nanocomposite	Used as catalyst during purification/separation reactions. Used in water treatment and medicine	[207]
Porous FeMnO	Supercapacitor electrode applications	[208]
Copper–porous silicon (Cu/PSi)	Can be used as an electrode as well as sensor for identifying formaldehyde during electrochemical applications	[209]

4 Conclusion

The research analyzed the synthesis, processing, preparation, and fabrication as well as elastic properties of FGP materials, along with the mathematical, numerical, and computational modeling. Manufacturing processes of every material differs naturally. One thing should be emphasized is that every material type including ceramics, metals, and polymer has a different processing technique for relative porous structures. However, the final fabrication method of both porous and nonporous structures is still the same after the raw material has been obtained *via* preprocessing. Additionally, sol–gel processing was found to be most popular processing technique for both porous and nonporous structures and it can be utilized for every type of nanocomposites (ceramic, metal, polymer). Metal nanocomposite structures are costly due to high temperature applications and production, whereas polymers are the most famous and chosen material for engineering application unless the application is an extreme temperature application. The addition of nano-reinforcing agents to the above-mentioned materials takes place during the synthesis and preparation, which were proven to enhance the mechanical and materialistic properties of the assemblies.

The effect of nanofillers of nanofillers were discussed and classified. The research highlighted the importance of nanofiller parameters on the elastic properties of the functionally graded nanocomposites. The tendencies found are as follows:

- Increasing the nanofiller composition in the structure increases the impact toughness of the nanocomposite and

Table 21: The classification of different modeling for beams

Nanocomposite type	Analysis type	Mathematical model	Numerical approach	Equation derivation method (including numerical method)	Computational algorithms used	Ref.
Beam	Static bending	GRF, Halpin–Tsai micromechanical along with the rule of mixtures	FEM	HSDT in matrix form solved by VDQ	Pseudo arc-length continuation algorithm	[15]
Beam	Thermal buckling	Halpin–Tsai micromechanical, GRF along with closed-cellular solids for matrices	FEM	Energy method and FSDT solved by GDQ	Not specified	[213,221,222]
Beam	Nonlinear free vibration and postbuckling analysis	Halpin–Tsai micromechanics along with rule of mixture	Not specified	Timoshenko beam theory and von Karman type arbitrary further solved by Ritz method	Direct iterative algorithm	[223,224]
Beam	Nonlinear flexural bending	Halpin–Tsai micromechanics	FEM	Shear deformation theory based on trigonometric function, von Karman, potential energy principle	Direct iteration algorithm	[225,226]
Beam	Dynamic instability	Halpin–Tsai micromechanics	Not specified	Differential quadrature method used to derive Mathieu–Hill equations, which was finally used together with Bolotin's method	Layer-wise model	[227,228]
Beams	Dynamic	Eshelby–Mori–Tanaka	FEM	Timoshenko and Euler–Bernoulli beam theories used, and equations derived *via* Hamilton's method together with Newmark's method	Not specified	[229]
Beams	Buckling and postbuckling	Halpin–Tsai micromechanics	Not specified	FSDT and differential quadrature method	Not specified	[230–232]
Multiwalled beams	Free and forced vibration	Not specified	FEM	Timoshenko beam theory	Not specified	[233]
Laminated beams	Bending stiffness and frequencies	Micromechanical	FEM	Karman type geometric nonlinearity and FSDT. Solved by differential quadrature technique	Not specified	[25,217]

Table 22: The classification of different modeling for plates

Nanocomposite type	Analysis type	Mathematical model	Numerical approach	Equation derivation method (including numerical method)	Computational algorithms used	Ref.
Plates	Free vibration	Halpin–Tsai along with rule of mixtures	FEM	FSDT	Layer-wise model	[234,235]
Plates	Thermoelastic	Eshelby–Mori–Tanaka	Not specified	Total energy function and two-plate theories	Mesh-free strategy	[17,236–238]
Plates	Transverse shear strain	Halpin–Tsai, rule of mixtures	Not specified	Chebyshev–Ritz method and FSDT	Not specified	[25]
Plates	3D free vibration and bending	Halpin–Tsai micromechanical model along with rule of mixtures	Not specified	State-space-based differential quadrature method	Not specified	[239]
Plates	Vibro-acoustic	Halpin–Tsai micromechanical	Not specified	Hamilton's principle and third-order shear deformation theory. Navier method and Rayleigh's method	Not specified	[240–242]
Plates	Statistical analysis including free vibration, mechanical properties	Halpin–Tsai micromechanical approach	FEM	HSDT	Analysis of variance used to derive empirical/ mathematical model	[243–245]
Plate	Control of nonlinear responses of piezoelectric FGP plates	Eshelby–Mori Tanaka	IGA	Bezier extraction and HSDT. Solved by Newton–Raphson iterative procedure and Newmark's time integration scheme	NURBS control meshing	[39,246–248]
Plate	Acoustic	Halpin–Tsai micromechanical with GRF	FEM	Hamilton's principle, Modal theory, and Rayleigh's integral method	Not specified	[26]
Plate	Bending and vibrational	Halpin–Tsai along with rule of mixtures	FEM	Not specified	Parametric study *via* FEM software	[249]
Quadrilateral plate	Nonlinear and free vibration	Classical plate theory	Not specified	Differential quadrature with transformed weighing coefficients. Von-Karman strain–displacement	Direct iterative algorithm ANSYS	[250–252]
Sandwich plates	Stress distributions/ forced vibration	Halpin–Tsai	FEM	FSDT MLSs and transformation technique	Mesh-free strategy MD	[214,253–255]

Table 23: The classification of different modeling for shells

Nanocomposite type	Analysis type	Mathematical model	Numerical approach	Equation derivation method (including numerical method)	Computational algorithms used	Ref.
Spherical shells	Free vibration and bending	Halpin–Tsai multiscale	Not specified	3D elasticity theory with state space method	Layer-wise analytical approach	[18]
Shells	Mechanical uncertainties on the free vibration properties	Halpin–Tsai micromechanical	FEM	HSDT solved *via* Fourier differential quadrature (FDQ)	Finite element analysis software ABAQUS	[256]
Conical shells	Free and nonlinear vibration	Not specified	Not specified	Hamilton's principle. FSDT, GDQM used to solve Donnel-type differential equations (DEs)	Parametric study	[257–261]
Cylindrical shells	Semianalytical postbuckling	Halpin–Tsai	Not specified	FSDT, von Karman, Fourier series and VDQ	Pseudo-arc length continuation and load disturbance approach	[262–265]
Cylindrical shells	Free vibration	Halpin–Tsai micromechanical along with rule of mixtures	Not specified	Hamilton's principle, FSDT	Parametric study	[258,266]
Shallow shells	Free vibration and static bending	Halpin–Tsai	FEM	Hamilton's principle, HSDT, Navier method	FEA software ANSYS	[267–269]
Cylindrical shells	Semianalytical wave characteristics	Halpin–Tsai along with rule of mixtures	Not specified	FSDT, higher order spectral elements, Hamilton's principle. Fourier transforms	Not specified	[270,271]
Shell	CNT added design	Eshebly–Mori–Tanaka	Not specified	Not specified	Mesh-free method and ONN	[215]
Double curved shallow shell/laminated composite plate	Free vibration and nonlinear dynamic response	Reddy's higher order	Finite element analysis	Shear deformation shell theory. Galerkin and fourth-order Runge–Kutta method FSDT	Not specified	[245,272–275]

Table 24: Key assumptions and the main distinctions of mechanical models

Mechanical modeling/equation derivation method	Brief explanation of theories, which are extensively used in studies	Ref.
Hamilton's principle	Assumes a system, which obeys Newtonian route and changes state from time to time Suitable for vibrational analysis. Used to derive elasticity and dynamic equations	[276]
Rule of mixtures	Utilized to predict properties of composite materials. Assumes properties of composites are functions of the volume-weighed mean of the matrices or distributed phase's properties	[277]
Halpin–Tsai	Utilized to estimate the elastic properties of composites by considering the topography and the arrangement of the filler (reinforcement) and the composite matrix. This method relies on Hartree–Fock system, which is also known as self-consistent system	[278,279]
Mori–Tanaka	An efficient field theory, which relies on Eshelby's elasticity approach for both inhomogeneous and infinite media. This method can be utilized to deduce mean internal stresses within a composite structure, which has inclusions due to strain variation. To be able to calculate the modulus of the nanocomposites, both matrix and the filler are required to have 3D elastic parameters	[279]
Runge–Kutta	An efficient strategy to resolve the initial value problems of DE. This approach can be utilized to develop higher order numerical method without requiring high-order derivatives	[280]
GDQM	Used to solve governing equations obtained from the mechanical modeling Produces efficient solutions especially for vibrational studies	[281]
FSDT	Used to perceive the impact of shear deformation on the structures. Assumes shear strain is constant throughout the thickness. Suitable for thinner structures	[282]
HSDT	Used to perceive the impact of shear deformation on the structures. Suitable for analysis of both thick and thin structures	

Young's modulus (E) of the soft/elastic nanocomposites. Contrarily, this will lead to a decrease in the Young's modulus values of hard/rigid porous nanocomposites.

- Increasing the amount of GPLs, increases buckling values and stiffness. Furthermore, it decreases static bending properties and led to an increase in interfacial stresses.
- Increasing the physical size of nanofillers, increases the Young's modulus (E) of porous structures.
- Decreasing the physical size of nanofillers, decreases the tensile strength of the porous structures.
- Endurance to bending can be increased when nanofillers are distributed uniformly.
- Square nanofillers distributed close to the top and the bottom of the beam structures increases stiffness and decreases deflection.
- Increasing the number of layers in laminated (sandwich) structures enhances the stress distribution.
- The physical proportion as well as the geometrical shape of the nanofiller greatly influences the bending properties. Increasing the height-over-length ratio of rectangular nanoporous filler increases deflection, increasing the thickness-over-length ratio of rectangular nanofiller decreases stiffness as well as deflection resistance.

The studies conducted to analyze various properties of porous nanocomposites includes broad mathematical and mechanical modeling assumptions. Modeling review highlighted some worth mentioned tendencies, which are specified below.

- Halpin–Tsai approach is the most common modeling type utilized in many applications including beams, plates, shells for many kinds of analysis including stress distribution, static bending, thermal buckling, thermoelastic, shear strain, vibrational, bending stiffness, and frequencies.
  - Rule of mixtures for composites, GRF, and micromechanical models are the methods used along with Halpin–Tsai.
- The most common numerical method used in FGM sector is FEM among reviewed studies.
- HSDT and FSFDT were the most common equation derivation methods.
  - In some cases, Chebyshev–Ritz method, total energy function, two-plate theory, energy functional method, 3D elasticity with state-space method, Karman type geometric nonlinearity, and Bezier extraction were used as well.
  - VDQ and GDQ approaches were the most common techniques to solve derived equations.

- Pseudo-arc length continuation algorithm, mesh-free strategy, layer-wise analytical approach, and MD approach were computer-aided methods used for analysis.
- NURBS control meshing optimization technique can be used along with iso geometric numerical method to control the nonlinear response of piezoelectric in FGP nanocomposite plates.

Apart from modeling and nanofiller properties, some other vital parameters were found that can greatly influence the operational lifetime and properties of the nanocomposites. These factors are given below.

- Elevated temperature and moisture led to the decrease in stiffness, natural frequency, and critical buckling load of porous nanocomposites.
- Functional grading of the core decreases deflection, which decreases flexibility.
- Elastic properties of the structure are greatly dependent on the CNF content distribution along the thickness direction of the assembly.
- Thermal residual stresses occurred during manufacturing, due to shrinkage and high temperature difference between operations, decreases the overall operational lifetime performance by increasing the interlaminar stresses.
- FGP nanocomposites with higher CNF content exhibits better flexural properties especially, higher stiffness.
  - Structures with higher CNF content have more tolerance to bending (flexible); however, toughness of such structures is naturally lower.
- Nongraded porous nanocomposites exhibit higher fracture load.
- Flexural strength and modulus are highly dependent on the direction of the exerted load.
  - Spherical nanoparticles offer higher flexural strength.
  - Nanorods offer higher flexural modulus to the structure.

Funding information: The authors state no funding involved.

Author contributions: All authors have accepted responsibility for the entire content of this manuscript and approved its submission.

Conflict of interest: The authors state no conflict of interest.

References

[1] Wu Q, Miao WS, Zhang YD, Gao HJ, Hui D. Mechanical properties of nanomaterials: a review. Nanotechnol Rev. 2020;9(1):259–73.

[2] Omanović-Mikličanin E, Badnjević A, Kazlagić A, Hajlovac M. Nanocomposites: a brief review. Health Technol (Berl). 2020;10(1):51–9.

[3] Ajayan PM, Pulickel M, Schadler LS, Linda S, Braun PV, Paul V. Bulk metal and ceramics. Nanocomposite science and technology. Vol. 230. Hoboken, New Jersey, United States of America: Wiley-VCH; 2003. p. 1–75.

[4] Bourchak M, Kada B, Alharbi M, Aljuhany K. Nanocomposites damage characterisation using finite element analysis. Int J Nanoparticles. 2009;2(1–6):467–75.

[5] Krasno S, Swathi K. A review on types of nanocomposites and their applications. Int J Adv Res Ideas Innov Technol. 2018;4(6):235–6. Available from: www.IJARIIT.com.

[6] Naebe M, Shirvanimoghaddam K. Functionally graded materials: a review of fabrication and properties. Appl Mater Today. 2016;5:223–45.

[7] Sola A, Bellucci D, Cannillo V. Functionally graded materials for orthopedic applications – an update on design and manufacturing. Biotechnol Adv. 2016;34(5):504–31.

[8] Gao K, Gao W, Chen D, Yang J. Nonlinear free vibration of functionally graded graphene platelets reinforced porous nanocomposite plates resting on elastic foundation. Compos Struct. 2018 Nov 15;204:831–46.

[9] Zhao S, Zhao Z, Yang Z, Ke LL, Kitipornchai S, Yang J. Functionally graded graphene reinforced composite structures: a review. Eng Struct. 2020;210:110339. doi: 10.1016/j.engstruct.2020.110339.

[10] Li Z. Exploration of the encased nanocomposites functionally graded porous arches: nonlinear analysis and stability behavior. Appl Math Model. 2020;82:1–16.

[11] Yang Z, Yang J, Liu A, Fu J. Nonlinear in-plane instability of functionally graded multilayer graphene reinforced composite shallow arches. Compos Struct. 2018;204(July):301–12. doi: 10.1016/j.compstruct.2018.07.072.

[12] Betts C. Benefits of metal foams and developments in modelling techniques to assess their materials behaviour: a review. Mater Sci Technol. 2012;28(2):129–43.

[13] Coskun S, Kim J, Toutanji H. Bending, free vibration, and buckling analysis of functionally graded porous micro-plates using a general third-order plate theory. J Compos Sci. 2019;3(1):15.

[14] Kiran MC, Kattimani SC. Assessment of porosity influence on vibration and static behaviour of functionally graded magneto-electro-elastic plate: a finite element study. Eur J Mech A/Solids. 2018;71:258–77.

[15] Yas MH, Rahimi S. Thermal buckling analysis of porous functionally graded nanocomposite beams reinforced by graphene platelets using generalized differential quadrature method. Aerosp Sci Technol. 2020;107:106261.

[16] Jalali MH, Zargar O, Baghani M. Size-dependent vibration analysis of fg microbeams in thermal environment based on modified couple stress theory. Iran J Sci Technol – Trans Mech Eng. 2019;43(s1):761–71. doi: 10.1007/s40997-018-0193-6.

[17] Safaei B, Moradi-Dastjerdi R, Behdinan K, Qin Z, Chu F. Thermoelastic behavior of sandwich plates with porous polymeric core and CNT clusters/polymer nanocomposite layers. Compos Struct. 2019;226:111209.

[18] Liu D, Zhou Y, Zhu J. On the free vibration and bending analysis of functionally graded nanocomposite spherical shells reinforced with graphene nanoplatelets: three-dimensional elasticity solutions. Eng Struct. 2021;226:111376.

[19] Wu H, Zhu J, Kitipornchai S, Wang Q, Ke LL, Yang J. Large amplitude vibration of functionally graded graphene nanocomposite annular plates in thermal environments. Compos Struct. 2020;239:112047.
[20] Bafekrpour E, Yang C, Natali M, Fox B. Functionally graded carbon nanofiber/phenolic nanocomposites and their mechanical properties. Compos Part A Appl Sci Manuf. 2013;54:124–34.
[21] Kumar S, Rath T, Mahaling RN, Reddy CS, Das CK, Pandey KN, et al. Study on mechanical, morphological and electrical properties of carbon nanofiber/polyetherimide composites. Mater Sci Eng B Solid-State Mater Adv Technol. 2007;141(1–2):61–70.
[22] Sun L, Gibson RF, Gordaninejad F, Suhr J. Energy absorption capability of nanocomposites: a review. Compos Sci Technol. 2009;69(14):2392–409.
[23] Patton RD, Pittman CU, Wang L, Hill JR. Vapor grown carbon fiber composites with epoxy and poly(phenylene sulfide) matrices. Compos Part A Appli Sci Manuf. 1999;30(9):1081–91.
[24] Mishra SK, Shukla DK, Patel RK. Effect of particle morphology on flexural properties of functionally graded epoxy-alumina polymer nanocomposite. Mater Res Express. 2019;6(12):250i9.
[25] Chen D, Yang J, Kitipornchai S. Nonlinear vibration and postbuckling of functionally graded graphene reinforced porous nanocomposite beams. Compos Sci Technol. 2017;142:235–45.
[26] Xu Z, Zhang Z, Wang J, Chen X, Huang Q. Acoustic analysis of functionally graded porous graphene reinforced nanocomposite plates based on a simple quasi-3D HSDT. Thin-Walled Struct. 2020;157:107151.
[27] Zhou Z, Ni Y, Tong Z, Zhu S, Sun J, Xu X. Accurate nonlinear buckling analysis of functionally graded porous graphene platelet reinforced composite cylindrical shells. Int J Mech Sci. 2019;151:537–50. doi: 10.1016/j.ijmecsci.2018.12.012.
[28] Mota AF, Loja MAR. Mechanical behavior of porous functionally graded nanocomposite materials. C. 2019;5(2):2–21.
[29] Liu H, Brinson LC. Reinforcing efficiency of nanoparticles: a simple comparison for polymer nanocomposites. Compos Sci Technol. 2008;68(6):1502–12.
[30] Viana JC. Polymeric materials for impact and energy dissipation. Plast Rubber Compos. 2006;35(6–7):260–7.
[31] Kireitseu M, Hui D, Tomlinson G. Advanced shock-resistant and vibration damping of nanoparticle-reinforced composite material. Compos Part B Eng. 2008;39(1):128–38.
[32] Cho J, Joshi MS, Sun CT. Effect of inclusion size on mechanical properties of polymeric composites with micro and nano particles. Compos Sci Technol. 2006;66(13):1941–52.
[33] Xu Y, Hoa SV. Mechanical properties of carbon fiber reinforced epoxy/clay nanocomposites. Compos Sci Technol. 2008;68(3–4):854–61.
[34] Polit O, Anant C, Anirudh B, Ganapathi M. Functionally graded graphene reinforced porous nanocomposite curved beams: bending and elastic stability using a higher-order model with thickness stretch effect. Compos Part B Eng. 2019;166:310–27.
[35] Yang Z, Feng C, Yang J, Wang Y, Lv J, Liu A, et al. Geometrically nonlinear buckling of graphene platelets reinforced dielectric composite (GPLRDC) arches with rotational end restraints. Aerosp Sci Technol. 2020;107:106326. doi: 10.1016/j.ast.2020.106326.
[36] Yang Z, Zhao S, Yang J, Lv J, Liu A, Fu J. In-plane and out-of-plane free vibrations of functionally graded composite arches with graphene reinforcements. Mech Adv Mater Struct. 2021;28(19):2046–56. doi: 10.1080/15376494.2020.1716420.
[37] Yang Z, Huang Y, Liu A, Fu J, Wu D. Nonlinear in-plane buckling of fixed shallow functionally graded graphene reinforced composite arches subjected to mechanical and thermal loading. Appl Math Model. 2019;70:315–27.
[38] Feng C, Kitipornchai S, Yang J. Nonlinear bending of polymer nanocomposite beams reinforced with non-uniformly distributed graphene platelets (GPLs). Compos Part B Eng. 2017;110:132–40.
[39] Nguyen NV, Nguyen LB, Lee J, Nguyen-Xuan H, Lee J. Analysis and active control of geometrically nonlinear responses of smart FG porous plates with graphene nanoplatelets reinforcement based on Bézier extraction of NURBS. Int J Mater Sci. 2019;180:105692.
[40] Arefi M, Firouzeh S, Mohammad-Rezaei Bidgoli E, Civalek Ö. Analysis of porous micro-plates reinforced with FG-GNPs based on Reddy plate theory. Compos Struct. 2020;247:112391.
[41] Bhat A, Budholiya S, Raj SA, Sultan MTH, Hui D, Shah AUM, et al. Review on nanocomposites based on aerospace applications. Nanotechnol Rev. 2021;10(1):237–53.
[42] Becher P. Microstructural design of toughened ceramics. J Am Ceram Soc. 1991;74(2):255–69.
[43] Yang Z, Xu J, Lu H, Lv J, Liu A, Fu J. Multiple equilibria and buckling of functionally graded graphene nanoplatelet-reinforced composite arches with pinned-fixed end. Crystals. 2020;10(11):1–13.
[44] Colombo P. Engineering porosity in polymer-derived ceramics. J Eur Ceram Soc. 2008;28(7):1389–95.
[45] Green D, Colombo P. Cellular ceramics: intriguing structures, novel properties, and innovative applications. MRS Bullettin. 2003;28:296–300.
[46] Messing GL, Stevenson AJ. Toward pore-free ceramics. Science. 2008;322(5900):381–3.
[47] Ohji T. Porous ceramic materials. Handbook of advanced ceramics: Materials, applications, processing, and properties. 2nd edn. Cambridge, Massachusetts, United States of America: Elsevier Inc; 2013. p. 1131–48.
[48] Liu P, Chen G. Fabricating porous ceramics. Porous Materials. Oxford, UK: Butterwoth-Heinemann; 2014. p. 221–302.
[49] Liu PS, Chen GF. General introduction to porous materials. Porous Materials. Oxford, UK: Butterwoth-Heinemann; 2014. p. 1–20.
[50] Gopi S, Pius A, Thomas S. Synthesis, microstructure, and properties of high-strength porous ceramics. Fundamental biomaterials: Ceramics. Sawston, Cambridge, United Kingdom: Elsevier Inc; 2018. p. 265–71.
[51] Ahmad R, Ha J-H, Song I-H. Processing methods for the preparation of porous ceramics. J Korean Powder Metall Inst. 2014;21(5):389–98.
[52] Liu P, Chen G. Producing polymer foams. Porous Materials. Oxford, UK: Butterwoth-Heinemann; 2014; p. 345–82.
[53] Hench LL, West JK. The sol–gel process. Chem Rev. 1990;90:33–72. https://pubs.acs.org/sharingguidelines.

[54] Baiju KV, Sibu CP, Rajesh K, Krishna Pillai P, Mukundan P, Warrier KGK, et al. An aqueous sol–gel route to synthesize nanosized lanthana-doped titania having an increased anatase phase stability for photocatalytic application. Mater Chem Phys. 2005;90(1):123–7.
[55] Henrique Cury Camargo P, Gundappa Satyanarayana K, Wypych F. Nanocomposites: synthesis, structure, properties and new application opportunities. Mater Res. 2009;12(1):1–39.
[56] Porwal H, Saggar R. Ceramic matrix nanocomposites. Comprehensive composite materials II. Amsterdam, Netherlands: Elsevier; 2017. p. 138–61.
[57] Wunderlich W, Padmaja P, Warrier KGK. TEM characterization of sol–gel-processed alumina-silica and alumina-titania nano-hybrid oxide catalysts. J Eur Ceram Soc. 2004;24(2):313–7.
[58] Riedel R, Seher M, Mayerd J. Vinga Szab3' D. polymer-derived s&based bulk ceramics, part I: preparation., processing and properties. J rhe Eur Ceram Sociefy. 1995;15:703–15.
[59] Gennari FC, Andrade-Gamboa JJ. A systematic approach to the synthesis, thermal stability and hydrogen storage properties of rare-earth borohydrides. Emerging materials for energy conversion and storage. Amsterdam, Netherlands: Elsevier; 2018. p. 429–59.
[60] Zhang Z, Du X, Wang J, Wang W, Wang Y, Fu Z. Synthesis and structural evolution of B_4C-SiC nanocomposite powders by mechanochemical processing and subsequent heat treatment. Powder Technol. 2014;254:131–6.
[61] Torabi O, Naghibi S, Golabgir MH, Tajizadegan H, Jamshidi A. Mechanochemical synthesis of NbC-NbB2 nanocomposite from the $Mg/B_2O_3/Nb/C$ powder mixtures. Ceram Int. 2015;41(4):5362–9.
[62] Sharifi EM, Karimzadeh F, Enayati MH. Preparation of Al_2O_3-TiB_2 nanocomposite powder by mechanochemical reaction between Al, B_2O_3 and Ti. Adv Powder Technol. 2011;22(4):526–31.
[63] Jamal Abbasi B, Zakeri M, Tayebifard SA. Mechanochemical synthesis of Al_2O_3-ZrB_2-ZrO_2 nanocomposite powder. Mater Res Bull. 2014;49(1):672–6.
[64] Fahami A, Nasiri-Tabrizi B, Ebrahimi-Kahrizsangi R. Synthesis of calcium phosphate-based composite nanopowders by mechanochemical process and subsequent thermal treatment. Ceram Int. 2012;38(8):6729–38.
[65] Palmero P. Structural ceramic nanocomposites: a review of properties and powders' synthesis methods. Nanomaterials. 2015;5(2):656–96.
[66] Choi S, Lee MS, Park DW. Photocatalytic performance of TiO_2/V_2O_5 nanocomposite powder prepared by DC arc plasma. Curr Appl Phys. 2014;14(3):433–8.
[67] Matović B, Yano T. Silicon carbide and other carbides: from stars to the advanced ceramics. Handbook of advanced ceramics: Materials, applications, processing, and properties. 2nd edn. Amsterdam, Netherlands: Elsevier Inc; 2013. p. 225–44.
[68] Sternitzke M. Review: structural ceramic nanocomposites. J Eur Ceram Soc. 1997;17:1061–82.
[69] Liu P, Chen G. Making porousmetals. Porous materials. Oxford, UK: Butterwoth-Heinemann; 2014. p. 21–112.
[70] Zaki ZI. Combustion synthesis of mullite-titanium boride composite. Ceram Int. 2009;35(2):673–8.
[71] Manukyan KV, Kharatyan SL, Blugan G, Kuebler J. Combustion synthesis and compaction of Si3N4-TiN composite powder. Ceram Int. 2007;33(3):379–83.
[72] Abovyan LS, Nersisyan HH, Kharatyan SL, Orruá R, Saiu R, Cao G, et al. Synthesis of alumina ± silicon carbide composites by chemically activated self-propagating reactions. Ceram Int. 2001;27:163–9.
[73] Ryu HY, Nersisyan HH, Lee JH. Preparation of zirconium-based ceramic and composite fine-grained powders. Int J Refract Met Hard Mater. 2012;30(1):133–8.
[74] Harra J, Nikkanen JP, Aromaa M, Suhonen H, Honkanen M, Salminen T, et al. Gas phase synthesis of encapsulated iron oxide-titanium dioxide composite nanoparticles by spray pyrolysis. Powder Technol. 2013;243:46–52.
[75] Tahmasebi K, Paydar MH. Microwave assisted solution combustion synthesis of alumina-zirconia, ZTA, nanocomposite powder. J Alloys Compd. 2011;509(4):1192–6.
[76] Reddy LH, Reddy GK, Devaiah D, Reddy BM. A rapid microwave-assisted solution combustion synthesis of CuO promoted CeO2-MxOy (M = Zr, La, Pr and Sm) catalysts for CO oxidation. Appl Catal A Gen. 2012 Nov 28;445–446:297–305.
[77] Chandradass J, Kim MH, Bae DS. Influence of citric acid to aluminium nitrate molar ratio on the combustion synthesis of alumina-zirconia nanopowders. J Alloys Compd. 2009;20:470(1–2):L9–12.
[78] Babooram K. Novel solution routes to ferroelectrics and relaxors. Handb Adv Dielectr Piezoelectric Ferroelectr Mater. 2008;1:852–83.
[79] Trandafir DL, Mirestean C, Turcu RVF, Frentiu B, Eniu D, Simon S. Structural characterization of nanostructured hydroxyapatite-iron oxide composites. Ceram Int. 2014;40(7B):11071–8.
[80] Wang H, Huang H, Liang J, Liu J. Preparation of ZrO_2/Gd_2O_3 composite ceramic materials by coprecipitation method. Ceram Int. 2014;40(3):3995–9.
[81] Han X, Liang Z, Feng L, Wang W, Chen J, Xue C, et al. Co-precipitated synthesis of Al2O3-ZrO2 composite ceramic nanopowders by precipitant and drying method regulation: a systematic study. Ceram Int. 2015;41(1):505–13.
[82] Palmero P, Naglieri V, Spina G, Lombardi M. Microstructural design and elaboration of multiphase ultra-fine ceramics. Ceram Int. 2011;37(1):139–44.
[83] Palmero P, Fornabaio M, Montanaro L, Reveron H, Esnouf C, Chevalier J. Towards long lasting zirconia-based composites for dental implants: part I: innovative synthesis, microstructural characterization and invitro stability. Biomaterials. 2015;50(1):38–46.
[84] Kern F, Palmero P, Marro FG, Mestra A. Processing of alumina-zirconia composites by surface modification route with enhanced hardness and wear resistance. Ceram Int. 2015;41(1):889–98.
[85] Yuan Z, Vleugels J, Van Der Biest O. Synthesis and characterisation of CeO-coated 2 ZrO powder-based TZP. Mater Lett. 2000;46:249–54.
[86] Chevalier J, Taddei P, Gremillard L, Deville S, Fantozzi G, Bartolomé JF, et al. Reliability assessment in advanced nanocomposite materials for orthopaedic applications. J Mech Behav Biomed Mater. 2011;4(3):303–14.

[87] Fornabaio M, Palmero P, Traverso R, Esnouf C, Reveron H, Chevalier J, et al. Zirconia-based composites for biomedical applications: role of second phases on composition, microstructure and zirconia transformability. J Eur Ceram Soc. 2015;35(14):4039–49.
[88] Mitra A, De G. Sol–gel synthesis of metal nanoparticle incorporated oxide films on glass. Glass nanocomposites: Synthesis, properties and applications. Norwich, New York, United States: Elsevier Inc; 2016. p. 145–63.
[89] Francis LF. Powder processes. In: Francis L, editor. Materials processing. 1st edn. Cambridge, Massachusetts, United States: Elsevier; 2016. p. 343–414.
[90] Joo SH, Nersisyan HH, Lee TH, Cho YH, Kim HM, Lee HH, et al. Effect of additives on the characteristics of amorphous nano boron powder fabricated by self-propagating high temperature synthesis. Korean J Mater Res. 2015;25(12):659–65.
[91] Gorup LF, Amorin LH, Camargo ER, Sequinel T, Cincotto FH, Biasotto G et al. Methods for design and fabrication of nanosensors: the case of ZnO-based nanosensor. In: Han B, Tomer VK, Singh PK, editors. Nanosensors for smart cities. 1st edn. Amsterdam, Netherlands: Elsevier; 2020. p. 9–30.
[92] Gavrilović TV, Jovanović DJ, Dramićanin MD. Synthesis of multifunctional inorganic materials: from micrometer to nanometer dimensions. In: Bhanvase BA, Pawade BV, Ashokkumar M, editors. Nanomaterials for green energy. Amsterdam, Netherlands: Elsevier; 2018. p. 55–81.
[93] Neikov OD. Production of aluminum alloy powders. Handbook of non-ferrous metal Powders. Amsterdam, Netherlands: Elsevier; 2019. p. 481–531.
[94] Stojanovic BD, Dzunuzovic AS, Ilic NI. Review of methods for the preparation of magnetic metal oxides. Magnetic, ferroelectric, and multiferroic metal oxides. Amsterdam, Netherlands: Elsevier; 2018. p. 333–59.
[95] Athar T. Smart precursors for smart nanoparticles. Emerging nanotechnologies for manufacturing. Norwich, New York, United States: Elsevier Science; 2014. p. 444–538.
[96] Liu S, Ma C, Ma MG, Xu F. Magnetic nanocomposite adsorbents. Composite nanoadsorbents. Amsterdam, Netherlands: Elsevier; 2018. p. 295–316.
[97] Rane AV, Kanny K, Abitha VK, Thomas S. Methods for synthesis of nanoparticles and fabrication of nanocomposites. Synthesis of inorganic nanomaterials. Sawston, Cambridge, United Kingdom: Elsevier; 2018. p. 121–39.
[98] Llorca-Isern N, Artieda-Guzmán C. Metal-based composite powders. Advances in powder metallurgy: Properties, processing and applications. Sawston, Cambridge, United Kingdom: Elsevier Inc; 2013. p. 241–72.
[99] Zhang JL, Hong GY. Nonstoichiometric compounds. Modern inorganic synthetic chemistry. 2nd edn. Amsterdam, Netherlands: Elsevier Inc; 2017. p. 329–54.
[100] Thostenson ET, Ren Z, Chou T-W. Advances in the science and technology of carbon nanotubes and their composites: a review. Comp Sci Technol. 2001;61(13):1899–921.
[101] Xia Z, Riester L, Curtin WA, Li H, Sheldon BW, Liang J, et al. Direct observation of toughening mechanisms in carbon nanotube ceramic matrix composites. Acta Mater. 2004 Feb 23;52(4):931–44.
[102] Kamalakaran R, Lupo F, Grobert N, Lozano-Castello D, Jin-Phillipp NY, Rühle M. In-situ formation of carbon nanotubes in an alumina-nanotube composite by spray pyrolysis. Carbon N Y. 2003;41(14):2737–41.
[103] An JW, You DH, Lim DS. Tribological properties of hot-pressed alumina-CNT composites. Wear. 2003;255(1–6):677–81.
[104] Jiang L, Gao L. Carbon nanotubes-magnetite nanocomposites from solvothermal processes: formation, characterization, and enhanced electrical properties. Chem Mater. 2003;15(14):2848–53.
[105] Torralba JM. Improvement of Mechanical and physical properties in powder metallurgy. Comprehensive materials processing. Amsterdam, Netherlands: Elsevier Ltd; 2014. p. 281–94.
[106] Madhuri KV. Thermal protection coatings of metal oxide powders. Metal oxide powder technologies. Amsterdam, Netherlands: Elsevier; 2020. p. 209–31.
[107] Dan A, Rachid A, Yann B, Rachid B, Charles K, Bruno C. Monolithic catalysts for the decomposition of energetic compounds. Stud Surf Sci Catlaysis. 2010;175:35–42.
[108] Goodall R, Mortensen A. Porous metals. In: Laughlin DE, Hono K, editors. Physical metallurgy. 5th edn. Amsterdam, Netherlands: Elsevier Inc; 2014. p. 2399–595.
[109] Banhart J. Manufacture, characterisation and application of cellular metals and metal foams. Prog Mater Sci. 2001;46:559–632.
[110] Liu PS, Chen GF. Making porousmetals. Porous materials. Oxford, UK: Butterwoth-Heinemann; 2014. p. 21–112.
[111] Hangai Y, Utsunomiya T, Hasegawa M. Effect of tool rotating rate on foaming properties of porous aluminum fabricated by using friction stir processing. J Mater Process Technol. 2010;210(2):288–92.
[112] Miyoshi T, Itoh M, Akiyama S, Kitahara A. ALPORAS aluminum foam: production process, properties, and applications. Adv Eng Mater. 2000;2(4):179–83.
[113] Hangai Y, Zushida K, Fujii H, Sun YF, Morisada Y, Kuwazuru O et al. Friction powder compaction process for fabricating porous Cu by space holder route. In: Fujii H, editor. Proceedings of the 1st International Joint Symposium on Joining and Welding; Osaka: Woodhead Publishing; Nov 6–8, 2013. p. 401–5.
[114] Hakamada M, Asao Y, Kuromura T, Chen Y, Kusuda H, Mabuchi M. Density dependence of the compressive properties of porous copper over a wide density range. Acta Mater. 2007;55(7):2291–9.
[115] Hassani A, Habibolahzadeh A, Bafti H. Production of graded aluminum foams *via* powder space holder technique. Mater Des. 2012;40:510–5.
[116] Pollien A, Conde Y, Pambaguian L, Mortensen A. Graded open-cell aluminium foam core sandwich beams. Mater Sci Eng A. 2005;404(1–2):9–18.
[117] Nakajima H. Fabrication, properties and application of porous metals with directional pores. Prog Mater Sci. 2007;52(7):1091–173.
[118] Kobashi M, Noguchi M, Kanetake N. Observation of foaming behavior for rolled sheet precursors made of various aluminum powders. Mater Trans. 2011;52(5):934–8.
[119] Shiomi M, Imagama S, Osakada K, Matsumoto R. Fabrication of aluminium foams from powder by hot extrusion and foaming. J Mater Process Technol. 2010;210(9):1203–8.
[120] Goodall DR. Porous metals: foams and sponges. Advances in powder metallurgy: Properties, processing and applications. Amsterdam, Netherlands: Elsevier Inc; 2013. p. 273–307.

[121] Technologies. P. Open vs. Closed Cell Foam. 2018 [cited 2021 Oct 31]. Available from: http://www.energsmart.com/spray-foam-insulation/open-vs-closed-cell-foam.html.
[122] Rahman MR, Hamdan SBin, Hossen MF. The effect of clay dispersion on polypropylene nanocomposites: physico-mechanical, thermal, morphological, and optical properties. In: Rahman MR, editor. Silica and clay dispersed polymer nanocomposites: Preparation, properties and applications. 1st edn. Sawston, Cambridge, United Kingdom: Elsevier; 2018. p. 201–57.
[123] Hihara LH, Bakkar A. Corrosion of metal matrix composites. Ref Modul Mater Sci Mater Eng. 1994;39(6):245–64.
[124] Dorin T, Vahid A, Lamb J. Aluminium lithium alloys. Lumley fundamentals of aluminium metallurgy. Sawston, Cambridge, United Kingdom: Elsevier; 2018. p. 387–438. Available from: https://linkinghub.elsevier.com/retrieve/pii/B9780081020630000114.
[125] Hong FJ, Qiu HH. Experimental study on rapid solidification process using a novel ultrasound technique. Exp Therm Fluid Sci. 2005;30(1):17–26.
[126] Behera A, Mallick P, Mohapatra SS. Nanocoatings for anticorrosion. In: Rajendran S, Nguyen T, Kakooei S, Yeganeh M, Li Y, editors. Corrosion protection at the nanoscale. 1st edn. Amsterdam, Netherlands: Elsevier; 2020. p. 227–43.
[127] Yilmaz E, Soylak M. Functionalized nanomaterials for sample preparation methods. In: Hussain CM, editor. Handbook of nanomaterials in analytical chemistry: Modern trends in analysis. Amsterdam, Netherlands: Elsevier; 2019. p. 375–413.
[128] Sakka Y, Hatton BD, Uchikoshi T. Processing of zirconia and alumina fine particles through electrophoretic deposition. Stud Surf Sci Catal. 2001;132:343–6.
[129] Sree Manu KM, Ajay Raag L, Rajan TPD, Gupta M, Pai BC. Liquid metal infiltration processing of metallic composites: a critical review. Metall Mater Trans B Process Metall Mater Process Sci. 2016;47(5):2799–819.
[130] Ambika S, Devasena M, Nambi IM. Synthesis, characterization and performance of high energy ball milled meso-scale zero valent iron in Fenton reaction. J Environ Manage. 2016;181:847–55.
[131] Faraji G. The ultrafine-grained and nanostructured materials. Severe plastic deformation. Amsterdam, Netherlands: Elsevier; 2018. p. 1–17.
[132] Edelstein AE. Nanomaterials. Encyclopedia of materials: Science and technology. 2nd edn. Washington: Elsevier; 2001. p. 5916–27.
[133] Shi D, Guo Z, Bedford N. Nanomagnetic materials. In: Shi D, editor. Nanomaterials and devices. Norwich, New York, United States: Elsevier; 2015. p. 105–59.
[134] Barua S, Geng X, Chen B. Graphene-based nanomaterials for healthcare applications. In: Choi SK, editor. Photonanotechnology for therapeutics and imaging. Amsterdam, Netherlands: Elsevier; 2020. p. 45–81.
[135] Dehghan Hamedan A, Shahmiri M. Production of A356-1wt% SiC nanocomposite by the modified stir casting method. Mater Sci Eng A. 2012;556:921–6.
[136] Sajjadi SA, Ezatpour HR, Beygi H. Microstructure and mechanical properties of Al-Al2O3 micro and nano composites fabricated by stir casting. Mater Sci Eng A. 2011;528(29–30):8765–71.
[137] Malaki M, Xu W, Kasar AK, Menezes PL, Dieringa H, Varma RS, et al. Advanced metal matrix nanocomposites. Metals (Basel). 2019;9(3):1–39.
[138] Goh CS, Wei J, Lee LC, Gupta M. Ductility improvement and fatigue studies in Mg-CNT nanocomposites. Compos Sci Technol. 2008;68(6):1432–9.
[139] Goh CS, Wei J, Lee LC, Gupta M. Properties and deformation behaviour of Mg-Y_2O_3 nanocomposites. Acta Mater. 2007;55(15):5115–21.
[140] Srivatsan TS, Godbole C, Paramsothy M, Gupta M. Influence of nano-sized carbon nanotube reinforcements on tensile deformation, cyclic fatigue, and final fracture behavior of a magnesium alloy. J Mater Sci. 2012;47(8):3621–38.
[141] De Cicco MP, Li X, Turng LS. Semi-solid casting (SSC) of zinc alloy nanocomposites. J Mater Process Technol. 2009;209(18–19):5881–5.
[142] Chaira D. Powder metallurgy routes for composite materials production. Reference module in materials science and materials engineering. Amsterdam, Netherlands: Elsevier; 2021.
[143] Nasiri Z, Sarkari Khorrami M, Mirzadeh H, Emamy M. Enhanced mechanical properties of as-cast Mg-Al-Ca magnesium alloys by friction stir processing. Mater Lett. 2021;296:129880.
[144] Bauri R, Yadav D, Suhas G. Effect of friction stir processing (FSP) on microstructure and properties of Al-TiC in situ composite. Mater Sci Eng A. 2011;528(13–14):4732–9.
[145] Saito Y, Utsunomiya H, Tsuji N, Sakai T. Accumulative roll-bonding. Acta Mater. 1999;47(2):579–83.
[146] Gupta M, Wong WLE. Magnesium-based nanocomposites: lightweight materials of the future. Mater Charact. 2015;105:30–46.
[147] Matli PR, Ubaid F, Shakoor RA, Parande G, Manakari V, Yusuf M, et al. Improved properties of Al-Si_3N_4 nanocomposites fabricated through a microwave sintering and hot extrusion process. RSC Adv. 2017;7(55):34401–10.
[148] Liao H, Chen J, Peng L, Han J, Yi H, Zheng F, et al. Fabrication and characterization of magnesium matrix composite processed by combination of friction stir processing and high-energy ball milling. Mater Sci Eng A. 2017;683:207–14.
[149] Alexandre M, Dubois P. Polymer-layered silicate nanocomposites: preparation, properties and uses of a new class of materials. Mater Sci Eng. 2000;28(1–2):1–63.
[150] Wu D, Xu F, Sun B, Fu R, He H, Matyjaszewski K. Design and preparation of porous polymers. Chem Rev. 2012;112(7):3959–4015.
[151] Berro S, El Ahdab R, Hajj Hassan H, Khachfe HM, Hajj-Hassan M. From plastic to silicone: the novelties in porous polymer fabrications. J Nanomater. 2015;2015(1):1–21.
[152] Coeli R, Dias M, Góes AM, Serakides R, Ayres E, Oréfice RL. Porous biodegradable polyurethane nanocomposites: preparation, characterization, and biocompatibility tests. Mater Res. 2010;13(2):211–8.
[153] Li B, Huang X, Liang L, Tan B. Synthesis of uniform microporous polymer nanoparticles and their applications for hydrogen storage. J Mater Chem. 2010;20(35):7444–50.
[154] Schacher F, Ulbricht M, Müller AHE. Self-supporting, double stimuli-responsive porous membranes from polystyrene-block-poly(N,N-dimethylaminoethyl methacrylate) diblock copolymers. Adv Funct Mater. 2009;19(7):1040–5.

[155] Manjooran NJ, Pickrell GR. Biologically self-assembled porous polymers. J Mater Process Technol. 2005;168(2):225–9.
[156] Xu Q. Nanoporous materials; synthesis and applications. In: Xu Q, editor. Nanoporous materials. 1st edn. Boca Raton, Florida, United States of America: CRC Press; 2013. p. 1–17.
[157] Thomas A, Goettmann F, Antonietti M. Hard templates for soft materials: creating nanostructured organic material. Chem Mater. 2008;20(3):738–55.
[158] Lynd NA, Meuler AJ, Hillmyer MA. Polydispersity and block copolymer self-assembly. Prog Polym Sci. 2008;33(9):875–93.
[159] Santos BAV, Silva VMTM, Loureiro JM, Rodrigues AE. Review for the Direct Synthesis of Dimethyl Carbonate. ChemBioEng Rev. 2014;1(5):214–29.
[160] Purkait MK, Sinha MK, Mondal P, Singh R. Introduction to Membranes. Interface science and technology. Amsterdam, Netherlands: Elsevier B.V; 2018. p. 1–37.
[161] Yabu H. Fabrication of honeycomb films by the breath figure technique and their applications. Sci Technol Adv Mater. 2018;19(1):802–22.
[162] Dhillon A, Kumar D. Recent advances and perspectives in polymer-based nanomaterials for Cr(VI) removal. In: Chaudhery MH, Mishra AK, editors. New polymer nanocomposites for environmental remediation. Amsterdam, Netherlands: Elsevier Inc; 2018. p. 29–46.
[163] Zaferani SH. Introduction of polymer-based nanocomposites. In: Jawaid M, Khan MM, editors. Polymer-based nanocomposites for energy and environmental applications: A volume in woodhead publishing series in composites science and engineering. Sawston, Cambridge, United Kingdom: University of Ottawa Press; 2018. p. 1–25.
[164] Hussain F, Hojjati M, Okamoto M, Gorga RE. Review article: polymer-matrix nanocomposites, processing, manufacturing, and application: an overview. J Compos Mater. 2006;40(17):1511–75.
[165] Biswas B, Bandyopadhyay NR, Sinha A. Mechanical and dynamic mechanical properties of unsaturated polyester resin-based composites. In: Sabu T, Hosur M, Chirayil CJ, editors. Unsaturated polyester resins: Fundamentals, design, fabrication, and applications. Amsterdam, Netherlands: Elsevier; 2019. p. 407–34.
[166] Asim M, Jawaid M, Saba N, Ramengmawii, Nasir M, Sultan MTH. Processing of hybrid polymer composites – a review. In: Thakur VK, Thakur MK, Gupta RK, editors. Hybrid polymer composite materials. Sawston, Cambridge, United Kingdom: Elsevier; 2017. p. 1–22.
[167] Devaraju S, Alagar M. Unsaturated polyester-macrocomposites. In: Thomas S, Hosur M, Chirayil CJ, editors. Unsaturated polyester resins: Fundamentals, design, fabrication, and applications. Amsterdam, Netherlands: Elsevier; 2019. p. 43–66.
[168] Kwon YW. Computational and experimental study of composite scarf bonded joints. Structural integrity and durability of advanced composites: Innovative modelling methods and intelligent design. Sawston, Cambridge, United Kingdom: Elsevier; 2015. p. 659–93.
[169] Erden S, Ho K. Fiber reinforced composites. In: Özgür Seydibeyoğlu M, Mohanty AK, Misra M, editors. Fiber technology for fiber-reinforced composites. Sawston, Cambridge, United Kingdom: Elsevier; 2017. p. 51–79.
[170] Smith RP, Qureshi Z, Scaife RJ, El-Dessouky HM. Limitations of processing carbon fibre reinforced plastic/polymer material using automated fibre placement technology. J Reinf Plast Compos. 2016;35(21):1527–42.
[171] Ouarhim W, Zari N, Bouhfid R, Qaiss AEK. Mechanical performance of natural fibers-based thermosetting composites. In: Mohammad J, Thariq M, Saba N, editors. Mechanical and physical testing of biocomposites, fibre-reinforced composites and hybrid composites. Sawston, Cambridge, United Kingdom: Elsevier; 2019. p. 43–60.
[172] McIlhagger A, Archer E, McIlhagger R. Manufacturing processes for composite materials and components for aerospace applications. In: Irving PE, Soutis C, editors. Polymer composites in the aerospace industry. Sawston, Cambridge, United Kingdom: Elsevier; 2014. p. 59–81.
[173] Raji M, Abdellaoui H, Essabir H, Kakou CA, Bouhfid R. El Kacem Qaiss A. Prediction of the cyclic durability of woven-hybrid composites. In: Mohammad J, Thariq M, Saba N, editors. Durability and life prediction in biocomposites, fibre-reinforced composites and hybrid composites. Sawston, Cambridge, United Kingdom: Elsevier; 2019. p. 27–62.
[174] Balasubramanian K, Sultan MTH, Rajeswari N. Manufacturing techniques of composites for aerospace applications. In: Jawaid M, Thariq M, editors. Sustainable composites for aerospace applications. Sawston, Cambridge, United Kingdom: Elsevier; 2018. p. 55–67.
[175] Ru-min W, Shui-Rong Z, Ya-Ping Z. Forming technology of polymer matrix composites. Polymer Matrix Composite Technology. Sawston, UK: Woodhead Publishing; 2011. p. 253–319, 547–8.
[176] Sandberg M, Yuksel O, Comminal RB, Sonne MR, Jabbari M, Larsen M et al. Numerical modeling of the mechanics of pultrusion. In: Vadim SV, editor. Mechanics of materials in modern manufacturing methods and processing techniques. Amsterdam, Netherlands: Elsevier; 2020. p. 173–95.
[177] Ngo T-D. Introduction to Composite Materials. Composite and nanocomposite materials. London, UK: Intech open; 2020. p. 1–27.
[178] Dai D, Fan M. Wood fibres as reinforcements in natural fibre composites: structure, properties, processing and applications. In: Hodzic A, Shanks R, editors. Natural fibre composites: Materials, processes and applications. Sawston, Cambridge, United Kingdom: Elsevier Inc.; 2013. p. 3–65.
[179] Hamidi YK, Yalcinkaya MA, Guloglu GE, Pishvar M, Amirkhosravi M, Altan MC. Silk as a natural reinforcement: processing and properties of silk/epoxy composite laminates. Materials (Basel). 2018;11(11):21–35.
[180] Quanjin M, Rejab MRM, Idris MS, Zhang B, Merzuki MNM, Kumar NM. Wireless technology applied in 3-axis filament winding machine control system using MIT app inventor. IOP Conference Series: Materials Science and Engineering, 2018 Oct 31; Pekan, Pahang. Malaysia: Institute of Physics Publishing; 2019. p. 12–30.
[181] Ma Q, Kumar NM, Quanjin M, Rejab RM, Zhang B. Filament winding technique: swot analysis and applied favorable factors additive manufacturing technique view project composite sandwich panel with novel contoured core view project filament winding technique: swot analysis and applied favorable factors. SCIREA J Mech Eng.

2019;3(1):15–23. Available from http://www.scirea.org/journal/Mechanical.
[182] Crosky A, Grant C, Kelly D, Legrand X, Pearce G. Fibre placement processes for composites manufacture. In: Philippe B, editor. Advances in composites manufacturing and process design. Sawston, Cambridge, United Kingdom: Elsevier Inc; 2015. p. 79–92.
[183] Hubert P, University M, Fernlund G, Poursartip A. Autoclave processing for composites. In: Advani SG, Hsiao K-T, editors. Manufacturing techniques for polymer matrix nanocomposites. Sawston, UK: Woodhead Publishing; 2012. p. 414–34.
[184] Campbell FC. Liquid molding: you get a good preform and tool. You get a good part. Manufacturing processes for advamced composites. Oxford, UK: Elsevier Advanced Technology; 2004. p. 303–56.
[185] Mouritz A. Manufacturing of fibre–polymer composite. In: Adrian PM, editor. Introduction to aerospace materials. Sawston, UK: Woodhead Publishing; 2012. p. 303–37.
[186] Pinkert K, Giebeler L, Herklotz M, Oswald S, Thomas J, Meier A, et al. Functionalised porous nanocomposites: a multidisciplinary approach to investigate designed structures for supercapacitor applications. J Mater Chem A. 2013;1(15):4904–10.
[187] Bhowmick A, Pramanik N, Mitra T, Gnanamani A, Das M, Kundu PP. Fabrication of porous magnetic nanocomposites for bone tissue engineering. New J Chem. 2016;41(1):190–7.
[188] Dadkhah M, Saboori A, Fino P. An overview of the recent developments in metal matrix nanocomposites reinforced by graphene. Materials (Basel). 2019;12(7):1944–96.
[189] Marouf BT, Bagheri R. Physical properties and applications of clay nanofiller/epoxy nanocomposites. In: Tjong SC, Mai Y-W, editors. Physical properties and applications of polymer nanocomposites. Sawston, Cambridge, United Kingdom: Woodhead Publishing Limited; 2010. p. 743–72.
[190] Kamalan Kirubaharan AM, Kuppusami P. Corrosion behavior of ceramic nanocomposite coatings at nanoscale. In: Rajendran S, Nguyen TA, Li Y, editors. Corrosion protection at the nanoscale. Amsterdam, Netherlands: Elsevier Inc; 2020. p. 295–314.
[191] Hu B, Qin X, Asiri AM, Alamry KA, Al-Youbi AO, Sun X. Synthesis of porous tubular C/MoS2 nanocomposites and their application as a novel electrode material for supercapacitors with excellent cycling stability. Electrochim Acta. 2013;100:24–8.
[192] Muthulakshmi L, Pavithra U, Sivaranjani V, Balasubramanian N, Sakthivel KM, Pruncu CI. A novel Ag/carrageenan–gelatin hybrid hydrogel nanocomposite and its biological applications: preparation and characterization. J Mech Behav Biomed Mater. 2021;115:104257.
[193] Sawada H. Preparation and applications of novel fluoroalkyl end-capped oligomeric nanocomposites. Polym Chem. 2012;3(1):46–65.
[194] Sarkar B. POSS-containing polyamide-based nanocomposites. In: Kalia S, Pielichowski K, editors. Polymer/POSS nanocomposites and hybrid materials: Preparation, properties, applications. Switzerland: Springer; 2018. p. 205–31.
[195] Thomas S, Stephen R. Rubber/Clay nanocomposites: preparation, properties, and applications. In: Thomas S, editor. Rubber nanocomposites. Hoboken, New Jersey, United States of America: John Wiley & Sons; 2010. p. 170–95.
[196] Chang H, Wu H. Graphene-based nanocomposites: preparation, functionalization, and energy and environmental applications. Energy Environ Sci. 2013;6(12):3483–507.
[197] Muhammed Shameem M, Sasikanth SM, Annamalai R, Ganapathi, Raman R. A brief review on polymer nanocomposites and its applications. Mater Today Proc. 2021;45(2):2536–9.
[198] Kim J, Kim TH, Lee JH, Park YA, Kang YJ, Ji HG. Porous nanocomposite of layered double hydroxide nanosheet and chitosan biopolymer for cosmetic carrier application. Appl Clay Sci. 2021;205:106067.
[199] Trnkova L, Triskova I, Cechal J, Farka Z. Polymer pencil leads as a porous nanocomposite graphite material for electrochemical applications: the impact of chemical and thermal treatments. Electrochem commun. 2021;126:107018.
[200] Sethi M, Shenoy US, Bhat DK. Simple solvothermal synthesis of porous graphene-NiO nanocomposites with high cyclic stability for supercapacitor application. J Alloys Compd. 2021;854:157190.
[201] Hussain MZ, Pawar GS, Huang Z, Tahir AA, Fischer RA, Zhu Y, et al. Porous ZnO/Carbon nanocomposites derived from metal organic frameworks for highly efficient photocatalytic applications – A correlational study. Carbon N Y. 2019;146:348–63.
[202] Luo W, Charara M, Saha MC, Liu Y. Fabrication and characterization of porous CNF/PDMS nanocomposites for sensing applications. Appl Nanosci. 2019;9(6):1309–17.
[203] Guo S, Lu G, Qiu S, Liu J, Wang X, He C, et al. Carbon-coated MnO microparticulate porous nanocomposites serving as anode materials with enhanced electrochemical performances. Nano Energy. 2014;9:41–9.
[204] Thakkar SV, Malfatti L. Silica-graphene porous nanocomposites for environmental remediation: a critical review. J Environ Manage. 2021;278:111519.
[205] Shen J, Chen X, Wang P, Zhou F, Lu L, Wang R, et al. Electrochemical performance of zinc carbodiimides based porous nanocomposites as supercapacitors. Appl Surf Sci. 2021;541:148355.
[206] Van Hoa N, Dat PA, Van Hieu N, Le TN, Minh NC, Van Tang N, et al. Rapid and efficient synthesis of high-porous reduced graphene oxide/NiCo2S4 nanocomposites for supercapacitor application. Diam Relat Mater. 2020;106:107850.
[207] Nsabimana A, Kitte SA, Wu F, Qi L, Liu Z, Zafar MN, et al. Multifunctional magnetic Fe 3 O 4/nitrogen-doped porous carbon nanocomposites for removal of dyes and sensing applications. Appl Surf Sci. 2019 Feb 15;467–468:89–97.
[208] Zhu G, Yang J, Liu Y, Xie X, Ji Z, Yin J, et al. Porous Fe-Mn-O nanocomposites: synthesis and supercapacitor electrode application. Prog Nat Sci Mater Int. 2016 Jun 1;26(3):264–70.
[209] Hajilari F, Farhadi K, Eskandari H, Allahnouri F. Application of Cu/porous silicon nanocomposite screen printed sensor for the determination of formaldehyde. Electrochim Acta. 2020;355:136751.
[210] Ansari R, Hassani R, Gholami R, Rouhi H. Nonlinear bending analysis of arbitrary-shaped porous nanocomposite plates using a novel numerical approach. Int J Non Linear Mech. 2020;126:103556.
[211] Arshid E, Amir S, Loghman A. Static and dynamic analyses of FG-GNPs reinforced porous nanocomposite annular

micro-plates based on MSGT. Int J Mech Sci. 2020;180:105656.
[212] Yang J, Chen D, Kitipornchai S. Buckling and free vibration analyses of functionally graded graphene reinforced porous nanocomposite plates based on Chebyshev-Ritz method. Compos Struct. 2018;193:281–94.
[213] Jalal M, Moradi-Dastjerdi R, Bidram M. Big data in nanocomposites: onn approach and mesh-free method for functionally graded carbon nanotube-reinforced composites. J Comput Des Eng. 2019;6(2):209–23.
[214] Moradi-Dastjerdi R, Aghadavoudi F. Static analysis of functionally graded nanocomposite sandwich plates reinforced by defected CNT. Compos Struct. 2018;200:839–48.
[215] Yaacoubi S, Dahmene F, Bouzenad A, El Mountassir M, Aouini M. Modal acoustic emission for composite structures health monitoring: issues to save computing time and algorithmic implementation. Compos Struct. 2018;183(1):338–46.
[216] Yang Z, Liu A, Yang J, Lai SK, Lv J, Fu J. Analytical prediction for nonlinear buckling of elastically supported fg-gplrc arches under a central point load. Materials (Basel). 2021;14(8):1–14.
[217] Song M, Gong Y, Yang J, Zhu W, Kitipornchai S. Nonlinear free vibration of cracked functionally graded graphene platelet-reinforced nanocomposite beams in thermal environments. J Sound Vib. 2020;468:115115.
[218] Zhao S, Yang Z, Kitipornchai S, Yang J. Dynamic instability of functionally graded porous arches reinforced by graphene platelets. Thin-Walled Struct. 2020;147:106491. doi: 10.1016/j.tws.2019.106491.
[219] Wu N, Wang Q, Pang SS. Dispersion of a bundle of carbon nanotubes by mechanical torsional energy. Carbon N Y. 2013;59:229–36. doi: 10.1016/j.carbon.2013.03.013.
[220] Bisheh H, Wu N. On dispersion relations in smart laminated fiber-reinforced composite membranes considering different piezoelectric coupling effects. J Low Freq Noise Vib Act Control. 2019;38(2):487–509.
[221] Jalali MH, Shahriari B, Zargar O, Baghani M, Baniassadi M. Free vibration analysis of rotating functionally graded annular disc of variable thickness using generalized differential quadrature method. Sci Iran. 2018;25(2B):728–40.
[222] Yang Z, Wu D, Yang J, Lai SK, Lv J, Liu A, et al. Dynamic buckling of rotationally restrained FG porous arches reinforced with graphene nanoplatelets under a uniform step load. Thin-Walled Struct. 2021;166:108103.
[223] Bartczak Z, Argon AS, Cohen RE, Weinberg M. Toughness mechanism in semi-crystalline polymer blends: II. High-density polyethylene toughened with calcium carbonate filler particles. Polymer (Guildf). 1999;40:2347–65.
[224] Xie B, Sahmani S, Safaei B, Xu B. Nonlinear secondary resonance of FG porous silicon nanobeams under periodic hard excitations based on surface elasticity theory. Eng Comput. 2021;37(2):1611–34. doi: 10.1007/s00366-019-00931-w.
[225] Anirudh B, Ben Zineb T, Polit O, Ganapathi M, Prateek G. Nonlinear bending of porous curved beams reinforced by functionally graded nanocomposite graphene platelets applying an efficient shear flexible finite element approach. Int J Non Linear Mech. 2020;119:103346.
[226] Yang Z, Lu H, Sahmani S, Safaei B. Isogeometric couple stress continuum-based linear and nonlinear flexural responses of functionally graded composite microplates with variable thickness. Arch Civ Mech Eng. 2021;21(3):1–19. doi: 10.1007/s43452-021-00264-w.
[227] Wu H, Yang J, Kitipornchai S. Dynamic instability of functionally graded multilayer graphene nanocomposite beams in thermal environment. Compos Struct. 2017;162:244–54.
[228] Li L, Luo Z, He F, Sun K, Yan X. An improved partial similitude method for dynamic characteristic of rotor systems based on Levenberg–Marquardt method. Mech Syst Signal Process. 2022;165(August 2021):108405. doi: 10.1016/j.ymssp.2021.108405.
[229] Yas MH, Heshmati M. Dynamic analysis of functionally graded nanocomposite beams reinforced by randomly oriented carbon nanotube under the action of moving load. Appl Math Model. 2012;36(4):1371–94.
[230] Yang J, Wu H, Kitipornchai S. Buckling and postbuckling of functionally graded multilayer graphene platelet-reinforced composite beams. Compos Struct. 2017;161:111–8.
[231] Yang Z, Liu A, Yang J, Fu J, Yang B. Dynamic buckling of functionally graded graphene nanoplatelets reinforced composite shallow arches under a step central point load. J Sound Vib. 2020;465:115019. doi: 10.1016/j.jsv.2019.115019.
[232] Safaei B, Naseradinmousavi P, Rahmani A. Development of an accurate molecular mechanics model for buckling behavior of multi-walled carbon nanotubes under axial compression. J Mol Graph Model. 2016;65:43–60. doi: 10.1016/j.jmgm.2016.02.001.
[233] Heshmati M, Yas MH. Vibrations of non-uniform functionally graded MWCNTs-polystyrene nanocomposite beams under action of moving load. Mater Des. 2013;46:206–18.
[234] Chiker Y, Bachene M, Guemana M, Attaf B, Rechak S. Free vibration analysis of multilayer functionally graded polymer nanocomposite plates reinforced with nonlinearly distributed carbon-based nanofillers using a layer-wise formulation model. Aerosp Sci Technol. 2020;104:105913.
[235] Safaei B, Ahmed NA, Fattahi AM. Free vibration analysis of polyethylene/CNT plates. Eur Phys J Plus. 2019;134(6):271–85.
[236] Safaei B, Moradi-Dastjerdi R, Qin Z, Behdinan K, Chu F. Determination of thermoelastic stress wave propagation in nanocomposite sandwich plates reinforced by clusters of carbon nanotubes. J Sandw Struct Mater. 2019;23:1–22.
[237] Fan F, Lei B, Sahmani S, Safaei B. On the surface elastic-based shear buckling characteristics of functionally graded composite skew nanoplates. Thin-Walled Struct. 2020;154:106841. doi: 10.1016/j.tws.2020.106841.
[238] Fan F, Cai X, Sahmani S, Safaei B. Isogeometric thermal postbuckling analysis of porous FGM quasi-3D nanoplates having cutouts with different shapes based upon surface stress elasticity. Compos Struct. 2021;262:113604. doi: 10.1016/j.compstruct.2021.113604.
[239] Liu D, Li Z, Kitipornchai S, Yang J. Three-dimensional free vibration and bending analyses of functionally graded graphene nanoplatelets-reinforced nanocomposite annular plates. Compos Struct. 2019;229:111453. doi: 10.1016/j.compstruct.2019.111453.

[240] Xu Z, Huang Q. Vibro-acoustic analysis of functionally graded graphene-reinforced nanocomposite laminated plates under thermal-mechanical loads. Eng Struct. 2019;186:345–55.
[241] Gao W, Qin Z, Chu F. Wave propagation in functionally graded porous plates reinforced with graphene platelets. Aerosp Sci Technol. 2020;102:105860. doi: 10.1016/j.ast.2020.105860.
[242] Shojaee M, Setoodeh AR, Malekzadeh P. Vibration of functionally graded CNTs-reinforced skewed cylindrical panels using a transformed differential quadrature method. Acta Mech. 2017;228(7):2691–711.
[243] Pashmforoush F. Statistical analysis on free vibration behavior of functionally graded nanocomposite plates reinforced by graphene platelets. Compos Struct. 2019;213:14–24.
[244] Moradi-Dastjerdi R, Behdinan K, Safaei B, Qin Z. Static performance of agglomerated CNT-reinforced porous plates bonded with piezoceramic faces. Int J Mech Sci. 2020;188:105966. doi: 10.1016/j.ijmecsci.2020.105966.
[245] Yuan Y, Zhao K, Sahmani S, Safaei B. Size-dependent shear buckling response of FGM skew nanoplates modeled via different homogenization schemes. Appl Math Mech (English Ed). 2020;41(4):587–604.
[246] Moradi-Dastjerdi R, Behdinan K, Safaei B, Qin Z. Buckling behavior of porous CNT-reinforced plates integrated between active piezoelectric layers. Eng Struct. 2020;222:111141. doi: 10.1016/j.engstruct.2020.111141.
[247] Moradi-Dastjerdi R, Behdinan K. Free vibration response of smart sandwich plates with porous CNT-reinforced and piezoelectric layers. Appl Math Model. 2021;96:66–79. doi: 10.1016/j.apm.2021.03.013.
[248] Moradi-Dastjerdi R, Behdinan K. Dynamic performance of piezoelectric energy harvesters with a multifunctional nanocomposite substrate. Appl Energy. 2021;293:116947. doi: 10.1016/j.apenergy.2021.116947.
[249] Zhao Z, Feng C, Wang Y, Yang J. Bending and vibration analysis of functionally graded trapezoidal nanocomposite plates reinforced with graphene nanoplatelets (GPLs). Compos Struct. 2017;180:799–808.
[250] Setoodeh AR, Shojaee M. Application of TW-DQ method to nonlinear free vibration analysis of FG carbon nanotube-reinforced composite quadrilateral plates. Thin-Walled Struct. 2016;108:1–11. doi: 10.1016/j.tws.2016.07.019.
[251] Setoodeh AR, Shojaee M, Malekzadeh P. Application of transformed differential quadrature to free vibration analysis of FG-CNTRC quadrilateral spherical panel with piezoelectric layers. Comput Methods Appl Mech Eng. 2018;335:510–37. doi: 10.1016/j.cma.2018.02.022.
[252] Fan F, Xu Y, Sahmani S, Safaei B. Modified couple stress-based geometrically nonlinear oscillations of porous functionally graded microplates using NURBS-based isogeometric approach. Comput Methods Appl Mech Eng. 2020;372:113400. doi: 10.1016/j.cma.2020.113400.
[253] Safaei B, Moradi-Dastjerdi R, Qin Z, Chu F. Frequency-dependent forced vibration analysis of nanocomposite sandwich plate under thermo-mechanical loads. Compos Part B Eng. 2019;161:44–54. doi: 10.1016/j.compositesb.2018.10.049.
[254] Safaei B. Frequency-dependent damped vibrations of multifunctional foam plates sandwiched and integrated by composite faces. Eur Phys J Plus. 2021;136(6):646. doi: 10.1140/epjp/s13360-021-01632-4.
[255] Fan F, Safaei B, Sahmani S. Buckling and postbuckling response of nonlocal strain gradient porous functionally graded micro/nano-plates *via* NURBS-based isogeometric analysis. Thin-Walled Struct. 2021;159:107231. doi: 10.1016/j.tws.2020.107231.
[256] Baghlani A, Najafgholipour MA, Khayat M. The influence of mechanical uncertainties on the free vibration of functionally graded graphene-reinforced porous nanocomposite shells of revolution. Eng Struct. 2021;228:111356. doi: 10.1016/j.engstruct.2020.111356.
[257] Rezaiee-Pajand M, Sobhani E, Masoodi AR. Free vibration analysis of functionally graded hybrid matrix/fiber nanocomposite conical shells using multiscale method. Aerosp Sci Technol. 2020;105:105998. doi: 10.1016/j.ast.2020.105998.
[258] Qin Z, Pang X, Safaei B, Chu F. Free vibration analysis of rotating functionally graded CNT reinforced composite cylindrical shells with arbitrary boundary conditions. Compos Struct. 2019;220:847–60. doi: 10.1016/j.compstruct.2019.04.046.
[259] Fattahi AM, Safaei B, Moaddab B. The application of nonlocal elasticity to determine vibrational behavior of FG nanoplates. Steel Compos Struct. 2019;32(2):281–92.
[260] Yuan Y, Zhao K, Han Y, Sahmani S, Safaei B. Nonlinear oscillations of composite conical microshells with in-plane heterogeneity based upon a couple stress-based shell model. Thin-Walled Struct. 2020;154:106857. doi: 10.1016/j.tws.2020.106857.
[261] Sahmani S, Safaei B. Large-amplitude oscillations of composite conical nanoshells with in-plane heterogeneity including surface stress effect. Appl Math Model. 2021;89:1792–813. doi: 10.1016/j.apm.2020.08.039.
[262] Ansari R, Torabi J. Semi-analytical postbuckling analysis of polymer nanocomposite cylindrical shells reinforced with functionally graded graphene platelets. Thin-Walled Struct. 2019;144:106248. doi: 10.1016/j.tws.2019.106248.
[263] Behdinan K, Moradi-Dastjerdi R, Safaei B, Qin Z, Chu F, Hui D. Graphene and CNT impact on heat transfer response of nanocomposite cylinders. Nanotechnol Rev. 2020;9(1):41–52.
[264] Yuan Y, Zhao K, Zhao Y, Sahmani S, Safaei B. Couple stress-based nonlinear buckling analysis of hydrostatic pressurized functionally graded composite conical microshells. Mech Mater. 2020;148:103507. doi: 10.1016/j.mechmat.2020.103507.
[265] Fattahi AM, Safaei B, Ahmed NA. A comparison for the non-classical plate model based on axial buckling of single-layered graphene sheets. Eur Phys J Plus. 2019;134(11):555.
[266] Dong YH, Li YH, Chen D, Yang J. Vibration characteristics of functionally graded graphene reinforced porous nanocomposite cylindrical shells with spinning motion. Compos Part B Eng. 2018;145:1–13.
[267] Wang A, Chen H, Hao Y, Zhang W. Vibration and bending behavior of functionally graded nanocomposite doubly-curved shallow shells reinforced by graphene nanoplatelets. Results Phys. 2018;9:550–9.
[268] Qin Z, Zhao S, Pang X, Safaei B, Chu F. A unified solution for vibration analysis of laminated functionally graded shallow shells reinforced by graphene with general boundary

conditions. Int J Mech Sci. 2020;170:105341. doi: 10.1016/j.ijmecsci.2019.105341.
[269] Safaei B, Fattahi AM. Free vibrational response of single-layered graphene sheets embedded in an elastic matrix using different nonlocal plate models. Mechanika. 2017;23(5):678–87.
[270] Li C, Han Q. Semi-analytical wave characteristics analysis of graphene-reinforced piezoelectric polymer nanocomposite cylindrical shells. Int J Mech Sci. 2020;186:105890. doi: 10.1016/j.ijmecsci.2020.105890.
[271] Qin Z, Safaei B, Pang X, Chu F. Traveling wave analysis of rotating functionally graded graphene platelet reinforced nanocomposite cylindrical shells with general boundary conditions. Results Phys. 2019;15:102752. doi: 10.1016/j.rinp.2019.102752.
[272] Duc ND, Hadavinia H, Quan TQ, Khoa ND. Free vibration and nonlinear dynamic response of imperfect nanocomposite FG-CNTRC double curved shallow shells in thermal environment. Eur J Mech A/Solids. 2019;75:355–66.
[273] Li Q, Xie B, Sahmani S, Safaei B. Surface stress effect on the nonlinear free vibrations of functionally graded composite nanoshells in the presence of modal interaction. J Brazilian Soc Mech Sci Eng. 2020;42(5):1–18. doi: 10.1007/s40430-020-02317-2.
[274] Safaei B, Fattahi AM, Chu F. Finite element study on elastic transition in platelet reinforced composites. Microsyst Technol. 2018;24(6):2663–71. doi: 10.1007/s00542-017-3651-y.
[275] Yuan Y, Zhao X, Zhao Y, Sahmani S, Safaei B. Dynamic stability of nonlocal strain gradient FGM truncated conical microshells integrated with magnetostrictive facesheets resting on a nonlinear viscoelastic foundation. Thin-Walled Struct. 2021;159:107249. doi: 10.1016/j.tws.2020.107249.
[276] Rosenhouse G. Basic principles. In: Braun S, editors. Vibration E of encyclopedia of vibration. United States of America: Academic Press; 2001. p. 124–37.
[277] Kopeliovich D. Estimations of composite materials properties. 2012 [cited 2021 Oct 29]. Available from: https://www.substech.com/dokuwiki/doku.php?id=estimations_of_composite_materials_properties.
[278] Halpin JC, editor. Effect of environmental factors on composite materials. 1st edn. Fort Belvoir, Virginia, United States of America: Defense Technical Information Center; 1969. p. 1–34.
[279] Shokrieh MM, Ghoreishi SM, Esmkhani M. Toughening mechanisms of nanoparticle-reinforced polymers. In: Qin Q, Ye J, editors. Toughening mechanisms in composite materials. Tehran: Woodhead Publishing Limited; 2015. p. 295–320.
[280] Zheng L, Zhang X. Numerical methods. In: Zheng L, Zhang X, editors. Modeling and analysis of modern fluid problems. Cambridge, Massachusetts, United States: Academic Press; 2017. p. 361–455.
[281] Gao F, Ren Y. Generalized differential quadrature method for free vibration analysis of a rotating composite thin-walled shaft. Math Probl Eng. 2019;2019:1538329. doi: 10.1155/2019/1538329.
[282] Thai H, Kim S. A simple higher-order shear deformation theory for bending and free vibration analysis of functionally graded plates. Compos Struct. 2013;96:165–73. doi: 10.1016/j.compstruct.2012.08.025.